Commercial Aircraft Trajectory Optimization and Efficiency of Air Traffic Control Procedures

A THESIS
SUBMITTED TO THE FACULTY OF THE GRADUATE SCHOOL
OF THE UNIVERSITY OF MINNESOTA
BY

Ryan Howe-Veenstra

IN PARTIAL FULFILLMENT OF THE REQUIREMENTS
FOR THE DEGREE OF
MASTER OF SCIENCE

Dr. Yiyuan J. Zhao

November, 2011

Acknowledgements

I would like to thank my research partner for this project Raghuveer Devalupalli for all of the hard work he put into this project to help us reach our goal. I would also like to thank Dr. Yiyuan J. Zhao and Dr. Michael R. Jackson for all of the assistance and support they provided.

Abstract

The Next Generation Air Traffic System (NextGen) offers a historical opportunity to re-examine the assumptions and constraints in the current Air Traffic Control (ATC) system and their effects on flight efficiency and safety. Modern day commercial aircraft are fully capable of flying continuously varying smooth trajectories. However in the current air traffic control ATC system, commercial flight trajectories consist of a series of segments due to historical development of navigation and surveillance systems. Segments are defined by one or more constant parameters such as Mach number or altitude. In this paper, characteristics and efficiencies of optimal free flights when ATC constraints are absent and optimal segmented flights in the current ATC system are compared. In this paper, aircraft flights are modeled as a point-mass. Both horizontal and vertical flight profiles are considered. Results of this paper seek to determine the potential benefit of supporting continuous trajectories in future ATC systems.

Contents

List of Tables

List of Figures

Chapter 1

Introduction

The demands on the commercial flight industry and its outdated Air Traffic Control (ATC) system have been rapidly increasing over the last decade. The ATC system has already exceeded its capacity, causing widespread flight delays during high demand periods, while passenger throughput is expected only to increase in the future, resulting in further stress on the ATC system. Coupled with the increasing demands on passenger and aircraft throughput, recent fuel trends have had a startling impact on the commercial flight industry. Fuel costs have been estimated at over half of the industry's total costs, forcing both commercial airline businesses and their consumers to share this burden. Additionally, the Federal Aviation Administration (FAA) has been pushing to make the commercial airline industry more environmentally safe by improving emissions and reducing noise.

The above factors result in an urgent need to improve the efficiency of the entire commercial airline industry and ATC system. The current ATC system is based on technology that was introduced in the 1960's and 70's and the available navigation tools of that time. While the system has evolved significantly over the many years, at its core it is still based on decades-old technology and does not fully utilize many of the modern navigational technologies such as GPS. The inability of old navigation technology to accurately measure true airspeed resulted in the use of flight segments which are often defined by constant calibrated airspeed (V_{CAS}) or Mach number. Airways defined by ground-based navigation beacons are still largely used to control traffic despite the ability to track continuous trajectories with modern technology. The ATC system has

also become very complex making it difficult to introduce new technologies or make modifications. Future ATC systems will need to be efficient and flexible so that another reconstruction of the ATC system is not required in another few decades. This system must result in improvements in fuel efficiency, safety, frequency of delays, and accuracy of trajectory prediction and tracking for both surface and air operations for it to truly be considered the next generation of Air Traffic Control.

While efficiency improvements have already been introduced through new navigation technology and aircraft design, such as Boeing's fuel efficient 787, implementation of a new ATC system is still in its early stages. Programs such as the FAA's NextGen[1] and Eurocontrol's Single European Sky ATM Research (SESAR) are leading the overhaul of the ATC system. Research is being conducted in all areas of Air Traffic Management (ATM) including flight scheduling, ground based trajectory planning, runway configuration, Automatic Dependent Surveillance-Broadcast (ADS-B), Flight Management Systems (FMS), and trajectory optimization with the goal of making these systems more automated and improving accuracy.

This paper will investigate discrete trajectory optimization algorithms and studies based on those algorithms in order to determine the potential impact of removing current ATC regulations on commercial flight efficiency. As previously stated, the current ATC system is based on dated technology, which also means the regulations and procedures that are in use are based on the same technology. Some of the restrictive ATC regulations are in place to maintain safety margins in spite of large uncertainties in older navigation tools, while others are due to the inability to accurately track trajectories. Modern navigation tools have incredible accuracy and allow for tracking of continuous trajectories, thus making it feasible to remove or significantly alter some of the restrictive ATC regulations on flight paths.

Many research efforts[2]-[16] have been conducted on commercial aircraft trajectory planning and prediction that pave the way for this work. In addition, classical aircraft performance studies[17]-[20] have examined steady-state climb and cruise flights with continuous variations of aircraft state. Optimal trajectory generations presented in this paper build on these excellent works and explicitly consider segmented flight structures enforced by ATC procedures. In addition, efforts are made for the systematic evaluation of generated trajectories. However, we have not seen statistical analyses studying the

benefits of using more densely populated waypoints to improve trajectory efficiencies.

A discussion of the ATC system and current ATC procedures is first presented, followed by a formulation of the commercial aircraft trajectory optimization problem using discrete search methods. Using the developed trajectory optimization algorithm, a comparison between trajectories which follow restrictive ATC procedures and those that are unrestricted is presented for vertical trajectories. In addition a statistical analysis of the above comparison is provided for horizontal trajectories in the presence of varying winds.

Chapter 2

Air Traffic Control Overview

A discussion of the structure of the United States ATC system along with the procedures and restrictions which it imposes on commercial flights will be presented in this chapter. This will include a brief overview of the different levels of the ATC system and a description of which sections of commercial flights they manage. Finally, a discussion of key ATC regulations and procedures relating to this paper will be presented for both horizontal and vertical trajectories.

2.1 ATC System Structure

A formulation of a standard commercial flight progressing through the ATC system will now be presented. The ATC system is divided into several sections of management, each of which is responsible for managing all aircraft within their region and handling the transfers of aircraft as they transition into or leave their region. Each section of the ATC system has unique responsibilities to the region they manage, but the primary duty of every region is to maintain safety and avoid incidents.

As the aircraft executes its ground operations leading to the runway, Ground Control determines the specific order aircraft will follow along with their surface trajectories. Ground Control's main objective is to manage ground flow and assure that incoming aircraft can efficiently vacate the runway area. From take-off until approximately 5 nm from the airport, the local Tower Control guides any aircraft within the region. Tower Control must manage the incoming and outgoing flows of aircraft and decide which

flight to give priority to in a variety of situations. Before leaving the Tower Control region, the aircraft is passed to Terminal Area Approach (TRACON) management which includes the region within roughly 40 nm of the airport. Another management level called En-Route Control or Center (ARTCC) manages trade-offs between TRACON's and aircraft above 18,000 ft. As the aircraft approaches its destination it enters a new Tower Control and then Ground Control after landing and completion of its route. Also of note, although not directly involved in specific flight procedures, ATC Systems Command Center analyzes nationwide aircraft flows in order to improve throughput efficiency.

The above represents the in-flight management portion of the ATC system, but additional sections of the ATC system provide other essential management assistance. Before departure, an airline flight dispatcher must determine a flight plan which must adhere to all ATC regulations and account for weather or other uncertain conditions. Flight planning will be discussed in more detail in Section 2.2. In addition to determining flight paths for individual aircraft, aircraft flows for the entire country are analyzed by the ATC Systems Command Center. The Command Center manages these flows with the goal of improving overall efficiency by focusing on optimizing the most congested regions.

2.2 ATC Regulations and Procedures

Numerous restrictions are imposed on the ATC system by the FAA which regulate every aspect of commercial flights. The primary purpose of these regulations is to maintain the safety of every aircraft whether on the ground or in the airspace. These include maintaining adequate separation between aircraft, limiting speed at lower altitudes where congestion is generally higher, maintaining speeds above stall velocity, and many other regulations which depend on the specifics of each flight. Passenger comfort and individual aircraft performance limitations also translate into ATC regulations on how quickly the aircraft can change its states, especially during cruise, and limits on maximum speed and ceiling altitude.

ATC regulations can be divided into two categories for the purpose of this paper:

those which impose rules on the interactions of two or more aircraft, and constraints applied to each individual flight plan. While the regulations on aircraft interactions are often the most important to maintain safety, for the purpose of studying single aircraft trajectories these regulations need not be discussed in further detail. The regulations imposed on individual flights can be translated into a general procedure which flight plans must adhere to.

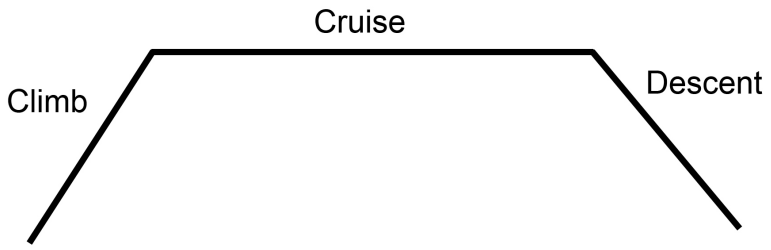

Figure 2.1: The three primary phases defining a commercial flight trajectory.

Commercial flights follow three phases: climb, cruise, and descent. Each of these phases may be divided into segments defined by certain constant parameters, such as a constant altitude and constant Mach cruise. Current flight planning methods break the trajectory into horizontal and vertical profiles, where the horizontal focuses on the lateral flight route, and the vertical depicts the variation of altitude versus total distance. Each profile is able to model different ATC procedures, such as the vertical profile's ability to model flight segments.

2.2.1 Horizontal Flight Planning

The horizontal flight plan depicts the constant Mach and constant altitude cruise phase of commercial flight providing East and North coordinates as functions of time. In the current ATC system, the cruise phase is not defined by a continuous path, but by a series of waypoints. Ideally waypoints are chosen to optimize efficiency in the presence of weather and other factors that influence route planning, but waypoints are located at pre-defined coordinates, which is sub-optimal when compared to a smooth continuous

trajectory.

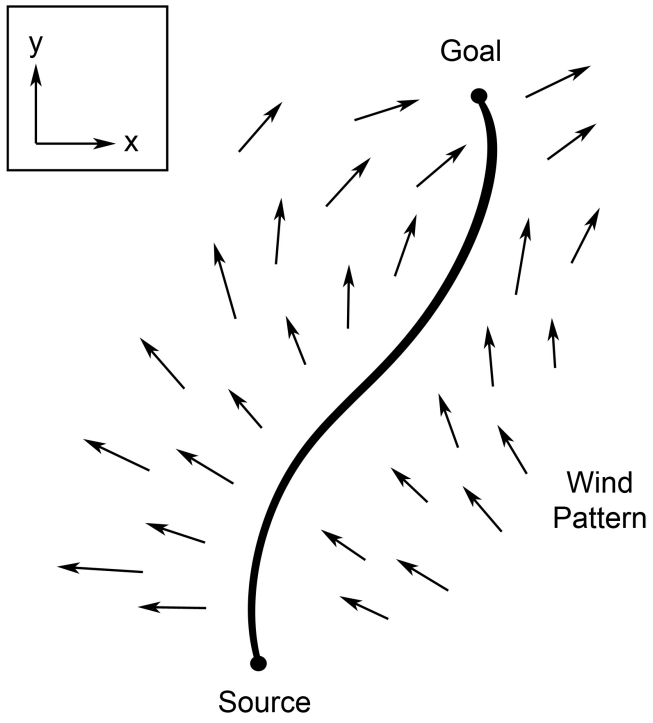

Figure 2.2: Example of a complete horizontal trajectory optimized for wind.

The most efficient cruise routes form continuous paths which are optimal in the presence of various weather conditions, but current ATC technology makes such a trajectory infeasible to plan or track. This provides motivation for NextGen to overhaul the ATC system. As each part of the ATC system interacts with another, dated technology in one portion of the ATC system will end up limiting the entire system. While a continuous optimal trajectory will be more efficient than any waypoint scheme, the comparison of benefits and costs in implementing such a method is the key deciding factor.

2.2.2 Vertical Flight Planning

A complete flight plan requires a vertical trajectory in addition to the described horizontal route. The vertical profile of an aircraft trajectory describes the altitude as a

function of total distance traveled. A majority of the ATC procedures relevant to this paper can only be modeled in the vertical portion of a trajectory, most of which are part of the descent phase. The restrictions imposed on each phase of an aircraft trajectory will now be presented in relation to the vertical profile.

The climb phase has fewer restrictions than other phases, and most also apply to the other phases. Upper and lower bounds are applied to flight path angle γ which are primarily to maintain passenger comfort and are also in effect throughout an entire flight. Another restriction imposed on the entire flight limits Calibrated Airspeed (V_{CAS}) below altitudes of $10,000$ ft to 250 knots or less. This regulation is safety related as it allows aircraft more maneuverability in the most densely occupied portions of the airspace where incidents are more likely to occur. Besides these universally applied restrictions, constant V_{CAS} and Mach segments typically define the climb phase.

As mentioned in the discussion of horizontal flight planning, the cruise phase is described by a constant slowly varying Mach number and constant altitude, although the constant altitude restriction is somewhat flexible. Sometimes aircraft are allowed to follow a step climb since it becomes more fuel efficient to increase altitude as the aircraft burns off fuel and reduces its mass. This is only allowed if it will not conflict with any nearby aircraft and the air traffic controller has sufficient time to verify the proposed change in altitude.

The final phase of a trajectory is the most restricted as the aircraft enters the congested region surrounding an airport. The descent phase is broken into several segments leading from the end of the cruise phase to the landing approach. For the studies provided in this paper, the landing approach will not be modeled, so the descent phase will be described up until the final runway approach.

The entire descent is considered to use idle thrust, but in practice a varying throttle will generally be required. As the cruise phase ends, the aircraft enters a constant altitude deceleration until it reaches its specified descent Mach number M_d, provided the descent Mach is less than the cruise Mach. This transitions into a constant Mach descent segment and is followed by a constant Calibrated Airspeed segment as the aircraft descends. At approximately $10,000$ ft the aircraft enters a constant altitude or shallow descent segment until it decelerates to a Calibrated Airspeed of 250 knots as is required under $10,000$ ft. The aircraft then maintains a Calibrated Airspeed of under

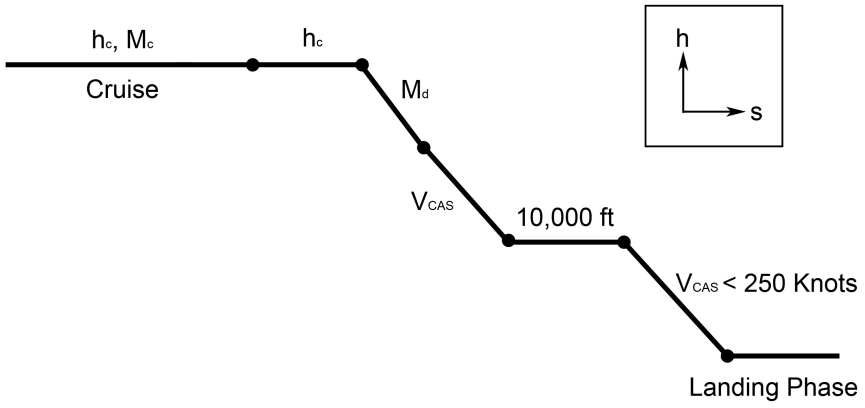

Figure 2.3: Typical structure of vertical descent phase.

250 knots until it descends to approximately $3,000$ ft where it begins the final landing approach.

Some of the above values will vary depending on the aircraft type, flight plan, or instructions provided by an air traffic controller. Ultimately, the current ATC procedures are quite restrictive and are far from optimal. While some of the restrictions are necessary to maintain safety, many of the restrictions imposed on individual flight plans are due to dated technology and the inability of the current ATC system to plan and track complete trajectories.

Chapter 3

Aircraft and Environment Modeling

Aircraft dynamic models[21] used to obtain the results provided in this thesis will be presented in this chapter. The point-mass aircraft model is assumed, and will be presented first in its general 3D form. This model will be completed by formulating motion constraints (Section 3.2) and detailing the performance models (Section 3.3). Given the complete model, extensions of the 3D point-mass model into horizontal and vertical models will be discussed. Finally, the environmental models for atmosphere and wind will be provided.

3.1 3D Point-Mass Aircraft Model

For the purposes of this study, the point-mass aircraft model has been assumed accurate enough to simulate trajectories of any typical commercial flights. Commercial aircraft change their direction and airspeed relatively slowly and typically follow flight paths which last on the order of an hour. Under these circumstances the point-mass model has been shown to accurately model aircraft flight with a desired simplicity which helps improve algorithm efficiency. The 3D point-mass aircraft model with horizontal directions x and y and vertical altitude h is as follows:

$$m\dot{V} = T \ - D - mg\sin\gamma - m\dot{W}_V \tag{3.1}$$

$$mV\cos\gamma\dot{\Psi} = L\sin\phi - m\dot{W}_{\Psi} \tag{3.2}$$

$$mV\dot{\gamma} = L\cos\phi - mg\cos\gamma + m\dot{W}_{\gamma} \tag{3.3}$$

$$\dot{x} = V\cos\gamma\sin\Psi + W_x \tag{3.4}$$

$$\dot{y} = V\cos\gamma\cos\Psi + W_y \tag{3.5}$$

$$\dot{h} = V\sin\gamma + W_h \tag{3.6}$$

These six equations represent the dynamic equations of motion governing the rate of change in velocity V, heading angle Ψ, flight path angle γ, East coordinate x, North coordinate y, and altitude h respectively. In addition to the above core dynamics the rate of change of mass for the aircraft, which translates to the amount of fuel burned, is modeled as a function of thrust and Thrust Specific Fuel Constant (TSFC).

$$\dot{m} = -\frac{c_{TSFC}}{g}T \tag{3.7}$$

The model for thrust is based upon the specific aircraft and its engine performance model which will be discussed in Section 3.3. Mach number is defined as

$$M = \frac{V}{a} \tag{3.8}$$

where a is the speed of sound at the aircraft's current altitude and temperature. Aircraft speed is also commonly commanded as Calibrated Airspeed (V_{CAS}) in the current ATC system which is defined as:

$$V_{CAS} = a_0\sqrt{5\left[\left(\frac{q_c}{p_{sl}}+1\right)^{\frac{2}{7}}-1\right]} \tag{3.9}$$

where a_0 is the speed of sound at 15° Celcius and q_c is the impact pressure or dynamic pressure as defined below.

$$q_c = p\left[\left(1+0.2M^2\right)^{\frac{7}{2}}-1\right] \tag{3.10}$$

Additional definitions of lift L and drag D are also required to complete the model.

$$L = \frac{1}{2}\rho V^2 S C_L \tag{3.11}$$

$$D = \frac{1}{2}\rho V^2 S(C_{D0} + KC_L^2) \tag{3.12}$$

These equations rely on both an atmospheric model (Section 3.5) as well as an aircraft performance model (Section 3.3) which describe the air density along with lift and drag coefficients.

Wind components can be described as the components along velocity, heading, and flight-path directions, but are most commonly described in terms of their East, North, and vertical components.

$$\dot{W}_V = \dot{W}_x \cos\gamma \sin\Psi + \dot{W}_y \cos\gamma \cos\Psi + \dot{W}_h \sin\gamma \tag{3.13}$$

$$\dot{W}_\Psi = \dot{W}_x \cos\Psi - \dot{W}_y \sin\Psi \tag{3.14}$$

$$\dot{W}_\gamma = \dot{W}_x \sin\gamma \sin\Psi + \dot{W}_y \sin\gamma \cos\Psi - \dot{W}_h \cos\gamma \tag{3.15}$$

3.2 Motion Constraints

Some motion constraints have been discussed in Section 2.2 in regards to their ATC origins, and further discussion will be presented in Section 4.4 where motion constraints relevant to the A* optimization algorithm will be introduced. In this section a complete formulation of all motion constraints will be provided which are based on aircraft limitations, ATC regulations, and passenger comfort.

Both flight path angle and rate of change of heading angle are constrained predominantly by passenger comfort

$$\gamma_{min} \leq \gamma \leq \gamma_{max} \tag{3.16}$$

$$|\dot{\Psi}| \leq \dot{\Psi}_{max} \tag{3.17}$$

while the limits on velocity are based on performance capabilities and safety. The lower bound on true airspeed and Calibrated Airspeed is the aircraft stall speed with an additional safety margin of 20%, and upper limits are defined by a Mach number lower than the maximum operating Mach value.

$$V \geq 1.2\sqrt{\frac{2mg}{\rho S C_{l_{max}}}} \tag{3.18}$$

$$M \leq M_{max} \tag{3.19}$$

Further constraints on Calibrated Airspeed are imposed by ATC regulations for aircraft below 10,000 ft.

$$V_{CAS} \leq 250 \text{ kts, for } h \leq 10,000 \text{ ft} \tag{3.20}$$

Aircraft performance defines limits of the lift coefficient and thrust

$$C_{l_{min}} \leq C_l \leq C_{l_{max}} \tag{3.21}$$

$$T_{min} \leq T \leq T_{max} \tag{3.22}$$

where the thrust constraints can be converted into constraints on acceleration, which will be useful in the A* search algorithm. Additionally, altitude is constrained by a maximum ceiling altitude, but is typically less restrictive than the constraints enforced by ATC.

$$h_{min} \leq h \leq h_{max} \tag{3.23}$$

3.3 Performance Model

Relevant performance modeling and specifications will be presented for the two aircraft types used in this thesis' results. The first model to be introduced was used for the vertical trajectory analysis, which is a generic small to medium sized transport aircraft model. For the horizontal trajectory, a Boeing 777-300 model was used to obtain results.

Both models share fundamental performance characteristics which will be presented first, including definitions of thrust, lift coefficient, and drag coefficient. The maximum available thrust is based on the maximum thrust at sea level and varies linearly with air density, meaning available thrust decreases as as the aircraft climbs. Minimum thrust is considered the idle thrust value.

$$T_{max} = \frac{\rho(h)}{\rho_{SL}} T_{max,SL} \tag{3.24}$$

$$T_{min} = T_{idle}(h) \tag{3.25}$$

The coefficient of drag is defined as:

$$C_D = C_{D_0}(M) + K(M)C_L^2 \tag{3.26}$$

which is a function of the parasitic drag coefficient, induced drag factor, and lift coefficient, and is thus also a function of Mach number.

3.3.1 Generic Aircraft Model

Accurate models of lift and drag coefficients were available for this generic aircraft model, which are typically unavailable for specific aircraft. Data representing these coefficients was provided by Wu el al [22] and is modeled as:

$$C_{D_0} = \begin{cases} 0.0123 & 0 < M < M_1 \\ 0.0123 - 0.0057z^2 + 0.158z^3 - 0.911z^4 + 1.6178z^5 & M_1 < M < M_{max} \end{cases} \tag{3.27}$$

$$K = \begin{cases} 0.06056 & 0 < M < M_1 \\ 0.06056 - 0.0707z^2 + 1.6097z^3 - 4.843z^4 + 6.4154z^5 & M_1 < M < M_{max} \end{cases} \tag{3.28}$$

$$C_{L_{max}} = \begin{cases} 1.8000 & 0 < M < M_1 \\ 1.8000 + 11.7z^2 - 317z^3 + 1432.7z^4 - 2018.8z^5 & M_1 < M < M_{max} \end{cases} \tag{3.29}$$

where $M_1 = 0.55$ and $z = M - M_1$

Additional values based on the aircraft's size, weight, and engine type are also required to complete the performance model. The take-off weight to wing area ratio, maximum sea level thrust to take-off weight, and TSFC are:

$$\frac{W_0}{S} = 120 \ lb/ft^2 \tag{3.30}$$

$$\frac{T_{max,SL}}{W_0} = 0.25 \tag{3.31}$$

$$c_{TSFC} = 0.725 \ lb/(h \ lbf) \tag{3.32}$$

based upon a total take-off weight of $W_0 = 10,000$ lb.

3.3.2 Boeing 777 Model

The lift and drag coefficients determined from available Boeing 777-300 aircraft data[23] are as follows:

$$C_{D_0} = 0.026 \tag{3.33}$$

$$K = 0.0431 \tag{3.34}$$

$$C_{L_{max}} = 1.8 \tag{3.35}$$

Take-off weight, wing area, TSFC, and maximum thrust at sea level are also provided:

$$W_0 = 217,700\ kg \tag{3.36}$$

$$S = 427.8\ m^2 \tag{3.37}$$

$$c_{TSFC} = 0.00001565\ \frac{kg}{N \cdot s} \tag{3.38}$$

$$T_{max,SL} = 830\ kN \tag{3.39}$$

The engine specifications are based on the Rolls-Royce Trent 892 model.

Figure 3.1: Boeing 777 Aircraft.

3.4 Horizontal and Vertical Profile Extension

In formulating the trajectory optimization problem as a discrete search, the 3D point-mass aircraft model was used as a starting point. Trajectory planning currently breaks down the flight path into its horizontal and vertical profiles, each of which are planned separately. This is inherently sub-optimal, but is a more computationally efficient approach to determining trajectories. A reduction of the 3D point-mass equations of motion into two 2D models, the horizontal and vertical profiles, will be presented along with the characteristics of each profile.

3.4.1 Horizontal Profile

The horizontal point-mass equations of motion are derived by eliminating flight path angle dynamics, i.e. setting $\gamma = 0$, which eliminates two equations from the 3D model and simplifies the remaining ones.

$$m\dot{V} = T - D - m\dot{W}_V \tag{3.40}$$

$$mV\dot{\Psi} = L\sin\phi - m\dot{W}_\Psi \tag{3.41}$$

$$\dot{x} = V\sin\Psi + W_x \tag{3.42}$$

$$\dot{y} = V\cos\Psi + W_y \tag{3.43}$$

$$\dot{W}_V = \dot{W}_x\sin\Psi + \dot{W}_y\cos\Psi \tag{3.44}$$

$$\dot{W}_\Psi = \dot{W}_x\cos\Psi - \dot{W}_y\sin\Psi \tag{3.45}$$

An additional equation is required which relates lift and bank angle to aircraft weight.

$$L\cos\phi = mg \tag{3.46}$$

This represents the constraint of constant altitude which is the key assumption for a horizontal profile.

Horizontal profiles focus on planning the cruise portion of commercial flight where the assumption of constant altitude remains valid. The goal in this paper of studying horizontal trajectories is to demonstrate the improvement in fuel efficiency possible by planning complete trajectories which take wind into account. While there are still vertical components of wind, they are generally smaller in magnitude than horizontal components and thus do not have as great an impact on cruise flight.

3.4.2 Vertical Profile

Starting from the 3D point-mass model again, removing heading angle and bank angle dynamics by setting $\Psi = 0$ and $\phi = 0$ results in the following vertical point-mass equations of motion.

$$m\dot{V} = T\ - D - mg\sin\gamma - m\dot{W}_V \tag{3.47}$$

$$mV\dot{\gamma} = L - mg\cos\gamma + m\dot{W}_\gamma \tag{3.48}$$

$$\dot{s} = V\cos\gamma + W_s \tag{3.49}$$

$$\dot{h} = V\sin\gamma + W_h \tag{3.50}$$

$$\dot{W}_V = \dot{W}_s\cos\gamma + \dot{W}_h\sin\gamma \tag{3.51}$$

$$\dot{W}_\gamma = \dot{W}_s\sin\gamma - \dot{W}_h\cos\gamma \tag{3.52}$$

Note that instead of using x and y to represent East and North horizontal components, they have been replaced by the total horizontal distance traveled s. The vertical profile can easily demonstrate the typical flight structure resulting from following ATC procedures, most notably the descent segments.

3.5 Atmosphere Model

Many aspects of the aircraft performance model also depend on atmospheric conditions resulting in a need for an accurate atmosphere model. Available thrust, lift, drag, and speed of sound all depend on the air density or temperature of the aircraft's current altitude. The importance of an accurate atmosphere model is increased when optimizing trajectories for fuel consumption since the aircraft will climb to a higher cruise altitude as the emphasis on fuel efficiency increases due to the reduction in drag.

The International Standard Atmosphere (ISA) model is presented for below and above the tropopause. The altitude of the tropopause can range from approximately 11 km at the Earth's poles to 17 km at the equator. The following are the temperature, pressure, and air density for altitudes below the tropopause ($h < h_T$):

$$\Theta_{ISA}(h) = \Theta_{SLS} + l_a h \tag{3.53}$$

$$\frac{p_{ISA}(h)}{p} = \left(1 + \frac{l_a h}{\Theta_{SLS}}\right)^{-\frac{g}{l_a R}} \tag{3.54}$$

$$\frac{\rho_{ISA}(h)}{\rho} = \left(1 + \frac{l_a h}{\Theta_{SLS}}\right)^{-\frac{g}{l_a R}-1} \tag{3.55}$$

and above the tropopause ($h > h_T$) temperature does not vary with altitude (for any altitude reachable by commercial aircraft).

$$\Theta_{ISA}(h) = \Theta_T \tag{3.56}$$

$$p_{ISA}(h) = p_T e^{-\frac{g}{R\Theta_T}(h-h_T)} \tag{3.57}$$

$$\frac{\rho_{ISA}(h)}{\rho} = \left(\frac{\Theta_T}{\Theta_{SLS}}\right)^{-\frac{g}{l_a R}-1} e^{-\frac{g}{R\Theta_T}(h-h_T)} \tag{3.58}$$

3.6 Wind Model

Wind models were used for the statistical analysis of horizontal trajectories as presented in Chapter 6. The wind models were determined by fitting historical wind data to 5th order polynomial functions of position. Wind data was provided by the National Operational Model Archive & Distribution System (NOAA), where data was taken from each day of the month of January, 2010. The data was first fit to polynomials as functions of geodetic latitude, longitude and altitude, and then converted into local flat-Earth coordinates for use in the trajectory optimization algorithm. These polynomials have been provided in Appendix B.

Chapter 4

Trajectory Optimization Formulation

4.1 Algorithm Selection

Several computer algorithms are able to solve trajectory optimization problems, most of which fall into one of two categories: continuous parameter optimization techniques and discrete search algorithms. Each category has inherent strengths and weaknesses which affect the type of algorithm that will best suit the desired formulation. Understanding the trade-offs between methods and which is best for a given problem formulation is key to deciding a solution strategy.

Continuous parameter optimization techniques are fairly efficient for basic trajectory optimization formulations with few additional constraints. The equations of motion are often redefined using discrete time steps in methods such as collocation. Then, starting from an initial guess the parameter optimization algorithm seeks to improve the guess by minimizing a performance index. The drawback to parameter optimization methods is that their runtime can increase drastically when more complicated constraints are implemented. These methods also tend be less flexible to changes in the problem formulation, depending on how much the formulations vary.

Discrete search strategies by comparison are very flexible to changes in the problem formulation and can also handle many constraints with ease, often decreasing the runtime of such algorithms. Two of the most common discrete search algorithms are

Dijkstra's algorithm and its heuristic based extension A Star (A*). These optimization algorithms work by defining a discrete search space and assigning costs to travel between intersection points. Then a search is conducted to determine the cost of all possible paths and the lowest-cost path is returned as the solution. The major drawback for discrete search algorithms is they can run out of memory and have large runtimes as the search dimensions and number of discrete intervals become large.

Since the main goal of the algorithm used in this project is that it has the ability to handle numerous constraints while maintaining flexibility, a discrete search algorithm was chosen to solve for optimal aircraft trajectories. The A* search algorithm was chosen for its previously mentioned use of a heuristic function. A heuristic function estimates the cost to reach the goal from the current location of the search. Under the condition that the heuristic cost is admissible, meaning it does not over-estimate the actual cost, it will reduce the number of points A* must search over in order to find the optimal solution. This translates into a reduction in runtime that is related to how close the heuristic estimate is to the actual cost without exceeding it.

4.2 Discrete Search Formulation

The foundation of a discrete search formulation is the construction of the search space, often referred to as the grid. This N-dimensional grid includes each of the N discretized search parameters as one dimension of the grid. Intersection points of the grid are referred to as nodes and represent specific pre-defined values of each search parameter. Discrete best-first search algorithms such as Dijkstra's or A* require the definition of the cost to travel from a given node to any other node along with an input defining the initial and final nodes of the desired path. Dijkstra's algorithm finds the optimal solution by calculating every possible path through the grid and storing the costs associated with them. Upon completion, it returns the path with the lowest cost as the optimal solution. As a best-first search algorithm, it does not calculate entire paths one at a time; rather it expands the search in a branching manner choosing the next most promising node, i.e. the one with the lowest cost to travel to.

Depending on how the user defines the search parameters, the nodes to which the algorithm may travel from a current node may be restricted in various ways. Search

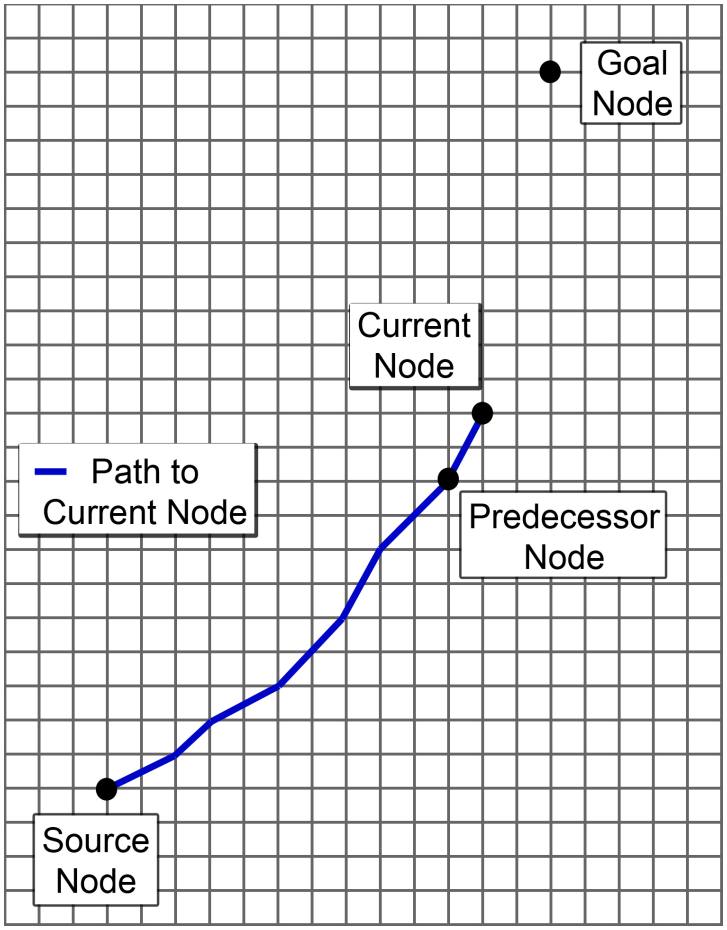

Figure 4.1: Example of a two-dimensional search grid and a path determined part way through a discrete search.

depth is the most general application of this restriction. Setting a search depth to a particular number, N_{sd}, will restrict the search to within N_{sd} search layers. All nodes within the search depth, or in a more general sense any node that the algorithm is allowed to travel from its current location, are considered the neighboring nodes. An example demonstrating search depth and search layers for a two-dimensional case has been provided.

The restriction of search nodes plays an important role in reducing the runtime of search algorithms. Specific methods of restricting nodes related to the trajectory

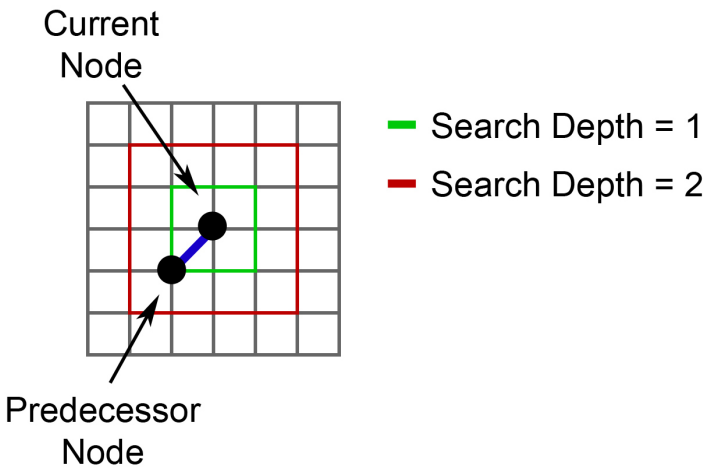

Figure 4.2: Definition of search depth for a two-dimensional grid.

optimization formulation will be discussed in Section 4.4.

While Dijkstra's algorithm is a complete search and therefore guarantees an optimal solution, it is inherently inefficient since is calculates every possible combination of paths from the source to goal. The A* algorithm, as previously discussed, guarantees the same optimal solution as Dijkstra's algorithm with the same or in most cases shorter runtime. This again is under the assumption that the heuristic function is admissible. The value of the heuristic function at a given node n, is the actual cost from the source to current node $g(n)$, plus the estimated cost from current node to goal $h(n)$.

$$f(n) = g(n) + h(n) \tag{4.1}$$

Thus with the correct choice of a heuristic function, A* is also a complete search guaranteeing an optimal solution, typically taking significantly less time than Dijkstra's algorithm.

To make use of the heuristic function in order to improve efficiency, A* stores relevant data from previously searched nodes in what is referred to as the open list. From the current node, all possible neighboring nodes are expanded and their heuristic costs are calculated and stored in the open list along with its preceding node. A* then chooses

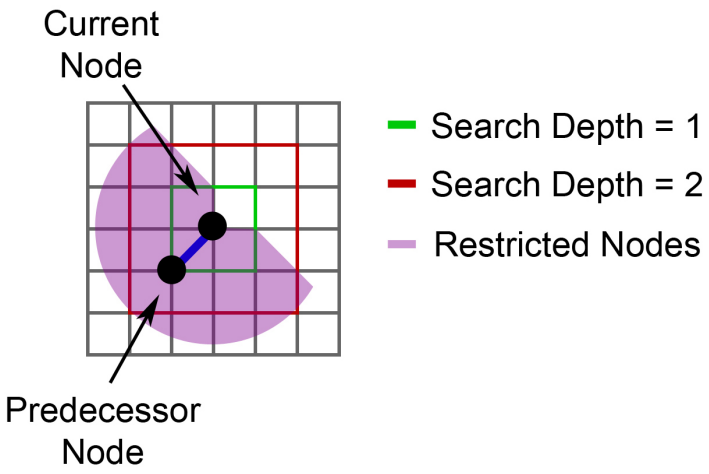

Figure 4.3: Demonstrates how nodes may be restricted in a two-dimensional grid.

the next node to evaluate by picking the node in the open list with lowest f value and then expanding its neighboring nodes. This process continues until the goal node has been expanded and has a lower f value than any other node in the open list. The optimal path is then determined by tracing back the path from the goal node to source, where each node in the path points to its predecessor. This is the method A* uses to reduce the number of expanded nodes required to determine the optimal solution.

A* continually accesses the open list in its search process as it selects the next node with lowest f value. This list can become incredibly large, especially for complex search spaces, and the search for the lowest f value node in the open list can become time consuming. Thus it is important to have the open list sorted each time newly expanded nodes are added. The binary heap method arranges the open list as new nodes are added so that the list is sorted by f value in descending order. Thus the lowest f value node is always at the top of the list, removing the need to search through the list.

4.3 Modeling ATC Procedures and Regulations

The modeling of ATC procedures and regulations is vital to this paper's goal of determining the potential benefit of removing certain ATC restrictions. ATC procedures, as discussed in Section 2.2, impose restrictions on commercial flight trajectories in a variety of ways. Some restrictions are rather simple to model, such as limiting Calibrated Airspeed to 250 knots or less for altitudes under $10,000$ ft, and can easily be implemented in most optimization algorithms. But modeling the segments of a trajectory, especially in the climb and descent phases, can can become difficult in many parameter optimization schemes. This leads to the key reason the A* search algorithm was chosen to determine optimal aircraft trajectories: its ability to incorporate many varying types of constraints with relative ease. This chapter will discuss the methods used to implement constraints imposed on single commercial aircraft trajectories within the context of a discrete search formulation.

4.3.1 Modeling Flight Segments

Flight segments can be modeled through the vertical profile most notably in the climb and descent phases of a trajectory. As discussed in Section 2.2, each segment is defined by one or more constant states of the aircraft such as altitude, Mach number, or Calibrated Airspeed, and also includes a condition to determine when each segment terminates. The segments form a logical progression; when one or more of the states which are allowed to vary reach certain values, the next segment begins and often holds those states constant. For example, a constant altitude deceleration segment may terminate once a certain Mach number has been reached, and then transition into a constant Mach descent segment.

Difficulties in modeling flight segments with discrete search algorithms result from the order these algorithms search through the grid. Flight segments follow a very specific order while the A* algorithm searches by expanding nodes in order of least cost, meaning that the order nodes are selected cannot be pre-determined. In order to simulate flight segments in the A* algorithm, it must record the the current segment number of each expanded node.

A separate algorithm has been constructed to model flight segments within the A*

discrete search formulation. Segments are labeled by integer values which point to the definition of each segment; so as a segment ends its segment number will increase by one. Each segment is defined in two parts, the set of parameters it may hold constant, and the terminating condition defining the end of the segment. Careful attention must be paid to the selection of terminating conditions so that they are feasible for all other constraints applied to the segment. Once the segments have been ordered and structured properly, the algorithm simply keeps track of the current segment of each expanded node. Then when a new node is expanded from a node in the open list, the algorithm first checks if the current segment has ended and then applies all constraints defined by the given segment.

4.4 A* Trajectory Optimization Implementation

In addition to the basic formulation of the A* discrete search algorithm, the following aspects must be defined specifically for the trajectory optimization problem: generation of the grid, definition of cost function and heuristic estimate of cost, and a choice of search depth or other restrictions on the search space. Once the above aspects have been accurately defined, A* will determine the optimal solution using the method described in Section 4.2.

The grid used with the 3D point-mass model includes three dimensions representing x, y, and h positions and another dimension for discretized velocity or Mach number. It is important for the search space to include a dimension representing Mach number or velocity due to the way A* stores node data. For example, if the search space were purely physical positions, then the algorithm would determine the locally optimal velocity to use when traveling from one node to another, but would not store any data for other velocities. When the path is traced backwards, it cannot return the globally optimal solution, only a combination of locally optimal solutions. Thus the algorithm needs data stored for all possible velocity divisions of each physical position in order to return a globally optimal solution. To complete the definition of the grid, the number of divisions for each dimension along with their corresponding step size must be defined. Discussions of factors to consider when choosing grid step sizes will be included in the following paragraphs.

Once the grid has been generated, a function which calculates the cost to travel from one node to another must be defined. It is desirable to optimize commercial aircraft trajectories based on a performance index which minimizes a combination of flight time and fuel consumption:

$$I = c_t t + c_f W_f \tag{4.2}$$

where c_t and c_f represent the respective weights for time and fuel consumption. Therefore, the function which calculates cost must determine the time and amount of fuel burned when traveling from the current node n_1 to another node n_2. Given the definition of the grid, complete information on position and velocity of both nodes is known by the cost function. The function can then input calculations from the aircraft performance model (Section 3.3) and atmospheric model (Section 3.5) to determine all other required values such as lift and drag coefficients, along with air density, pressure, and temperature. Further calculations include heading angle Ψ and flight path angle γ which are interpreted from the physical positions of n_1 and n_2. One key assumption is made during this portion of the algorithm: that velocity varies linearly between nodes n_1 and n_2. This assumption improves algorithm efficiency and reduces its complexity while maintaining sufficient accuracy when the time scale is on the order of several seconds. Since commercial aircraft change their states relatively slowly, the linearly varying velocity assumption holds quite well over periods of several seconds. It is important to note that this is one of the deciding factors when choosing the spacing between nodes in order to maintain accuracy. Finally, time and fuel consumption are calculated by numerical integration and the cost to travel from node n_1 to n_2 can be determined.

Now that the algorithm can calculate the cost from a current node to any other node, a meaningful formulation of how the algorithm limits which nodes it can select from its current node is desired. First, many surrounding nodes can be eliminated as possibilities by imposing aircraft performance constraints. Limits on flight path angle, rate of change of heading angle, and acceleration can significantly reduce runtime by limiting the number of nodes A* needs to search over (eqs. 3.16, 3.17, and **??**). Secondly, the search depth N_{sd} must be chosen carefully to achieve a balance of performance and accuracy of the solution. If the x and y grid spacings are equal, then setting $N_{sd} = 1$ will result in heading angles which are multiples of 45°. This will not provide an accurate solution, so a higher search depth is required. However, as the search depth increases

the runtime increases significantly, meaning the correct balance between accuracy and runtime must be chosen based on the results desired. Search depth also affects the choice of grid spacings for physical search dimensions as they must be chosen so that the aircraft has a reasonable number of nodes it may travel to from its current node.

Chapter 5

Vertical Trajectory Analysis

The results presented in this chapter will focus on demonstrating the flexibility of the A* algorithm. Vertical commercial aircraft trajectories provide the opportunity to incorporate a variety of physical and procedural constraints into a single simulation. Trajectories following the ATC constraints and procedures discussed in Chapter 2 will be presented and then compared to unrestricted trajectories. A discussion of the potential benefits of removing these restrictions on the vertical components of commercial flight will be discussed for the descent phase, and then entire trajectories. First, a discussion on the feasibility of removing ATC restrictions relating to vertical trajectory planning will be presented.

5.1 Feasibility of Removing ATC Restrictions

The significance of any demonstrated benefit of removing ATC restrictions on commercial flight depends on the feasibility of removing those restrictions. If the improvements in efficiency are based on removing ATC regulations required to maintain safety, then the results warrant little consideration. The feasibility of removing ATC restrictions will be analyzed by considering the technological and procedural changes proposed by NextGen. If the implementation and integration of modern navigation and tracking technology can remove the need for a given restriction while maintaining safety, the removal of said restriction will be considered feasible.

The ability to plan efficient trajectories that take weather conditions into account

is important to the future of the commercial airline industry. Many options are available for flight planning methods which provide more efficient trajectories than methods currently used by the ATC system. Many flight planning algorithms are available today which provide efficient trajectories and can incorporate more accurate wind models into the planning process. The runtime of these trajectory planning algorithms is one concern, especially with the desire to plan flights as full 4D trajectories (three physical search dimensions along with one for speed or time). One proposed solution to potential runtime issues is to use databases of pre-defined trajectories based on various wind patterns[24]. This would allow for near instant route planning with the drawback that routes will not be completely tailored to the specifics of each flight. While there are advantages and disadvantages of each method, ultimately the ability to plan more efficient trajectories exists with present day technology.

ATC restrictions applied to vertical trajectories primarily rely on the ability to track and effectively manage numerous aircraft in a given airspace. This is especially true in regions surrounding airports where many arrivals and departures must be managed with safety as the highest priority. Accurate and reliable tracking technology exists, but is not currently fully integrated into the ATC system. This results in the need to maintain large spacings between aircraft in the presence of tracking uncertainties and lack of additional automated traffic management tools. Commercial aircraft currently have the ability to fly Continuous Descent Approaches (CDA) which are faster and more fuel efficient than the typical segmented descent, but the dated ATC system is preventing these approaches from becoming the standard. Additionally, ATC procedures restrict the speed of aircraft under $10,000$ ft to a 250 knot Calibrated Airspeed or less to maintain safety in the presence of tracking and aircraft management uncertainty. This restriction is also enforced to reduce the noise in terminal areas, meaning some form of a low altitude speed limit would likely still be enforced in future ATC systems, but it would have the ability to be more flexible. Future improvements to the ATC system should greatly improve the management and tracking of aircraft, thus providing the opportunity to remove or reduce low altitude speed limits and allow operations such as CDA's to become routine.

The same fundamental ATC issues that currently prevent aircraft from flying optimal descent procedures also limit their operations during cruise. As mentioned in

Section 2.2.2, commercial aircraft are sometimes allowed to perform a step climb during cruise, but this is dependent on the locations and routes of nearby aircraft as well as the workload of controllers (step climbs are not a priority task for air traffic controllers). Proposed future improvements to the cruise portions of flight include the implementations of Trajectory Based Operations (TBO). With TBO aircraft would be cleared to fly within a pre-defined tube of airspace rather than a specific route of waypoint and altitude coordinates. This would allow for aircraft to perform step climbs or even continuous gradual climbs during cruise without requiring a controller's approval.

5.2 Descent Phase Analysis

Under the assumption that it will be feasible to follow a CDA procedure and minimize low altitude speed limits in future ATC systems as discussed in Section 5.1, a comparison between restricted and unrestricted descent trajectories will now be presented. Since the descent phase is the most restricted phase of commercial flight, one would predict it has the potential to demonstrate significant improvements in efficiency by removing unnecessary ATC restrictions. The following results compare the descent phases of restricted and unrestricted trajectories under the below conditions. Limits on maximum and minimum cruise Mach number and flight path angle are:

$$0.25 \leq M \leq 0.8 \tag{5.1}$$

$$-3^{\circ} \leq \gamma \leq 8^{\circ} \tag{5.2}$$

Note that the minimum Mach number is the value used to determine the Mach dimension search spacings; the actual minimum is calculated dynamically. Gross take-off weight for this generic small to medium sized commercial aircraft is:

$$W_0 = 45,360\ kg \tag{5.3}$$

The grid was formed using 1,000 divisions in the s direction, 250 vertical h divisions, and 100 Mach divisions with the following horizontal and vertical spacings:

$$\Delta s = 1000\ meters \tag{5.4}$$

$$\Delta h = 50\ meters \tag{5.5}$$

The search depth used for these simulations was:

$$N_d = 2 \tag{5.6}$$

Finally, the performance index used for the provided results is as follows:

$$I = c_t t + c_f m_f \tag{5.7}$$

$$c_t = 0.1 \tag{5.8}$$

$$c_f = 1 \tag{5.9}$$

where time was measured in units of seconds and fuel consumption in kg.

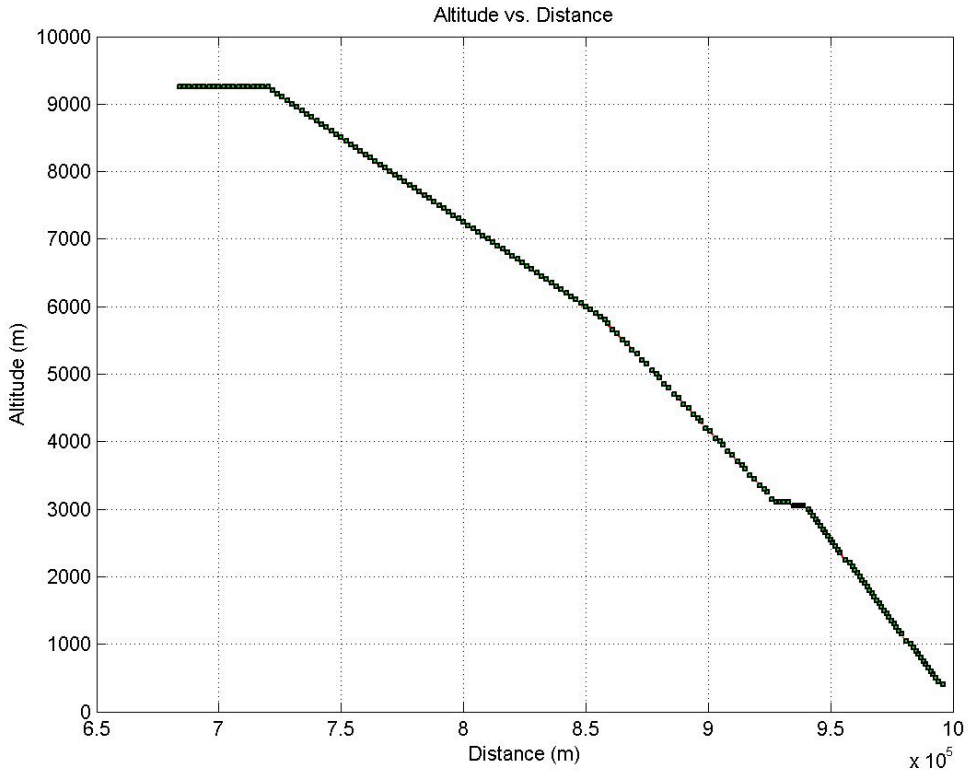

Figure 5.1: Restricted Descent Phase: Altitude vs. Distance.

The first set of results shows a descent phase restricted by ATC procedures. Figures 5.1, 5.2, and 5.3 depict altitude, Mach number, and V_{CAS} as functions of horizontal distance. The aircraft can be verified to follow typical ATC descent procedures as described in figure 2.3 including the constant altitude deceleration, constant Mach descent, constant V_{CAS} descent, and the second constant altitude deceleration.

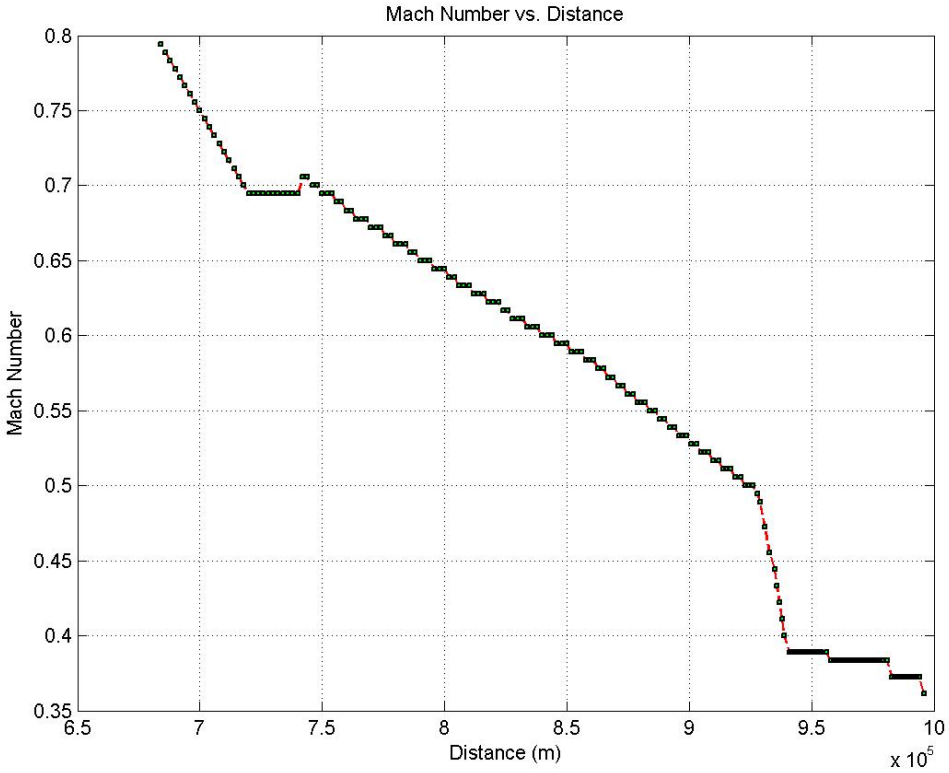

Figure 5.2: Restricted Descent Phase: Mach Number vs. Distance.

The values for the constant Mach and V_{CAS} segments respectively are:

$$M_d = 0.7 \tag{5.10}$$

$$V_{CAS_d} = 140\ m/s\ (272\ knots) \tag{5.11}$$

In the Calibrated Airspeed plot, the V_{CAS} oscillates around the V_{CAS_d} value; this is due to Mach number being the variable chosen as the speed search dimension. Despite

the constraints on this descent phase, the search algorithm is still optimizing over any parameter that has not been held constant, so this is still an optimal solution given the constraints. These results demonstrate the flexibility discrete search algorithms can bring to trajectory optimization. Not only can the algorithm easily incorporate a variety of complex procedures and constraints, the more heavily constrained a discrete search is, the more efficiently it finds the optimal solution.

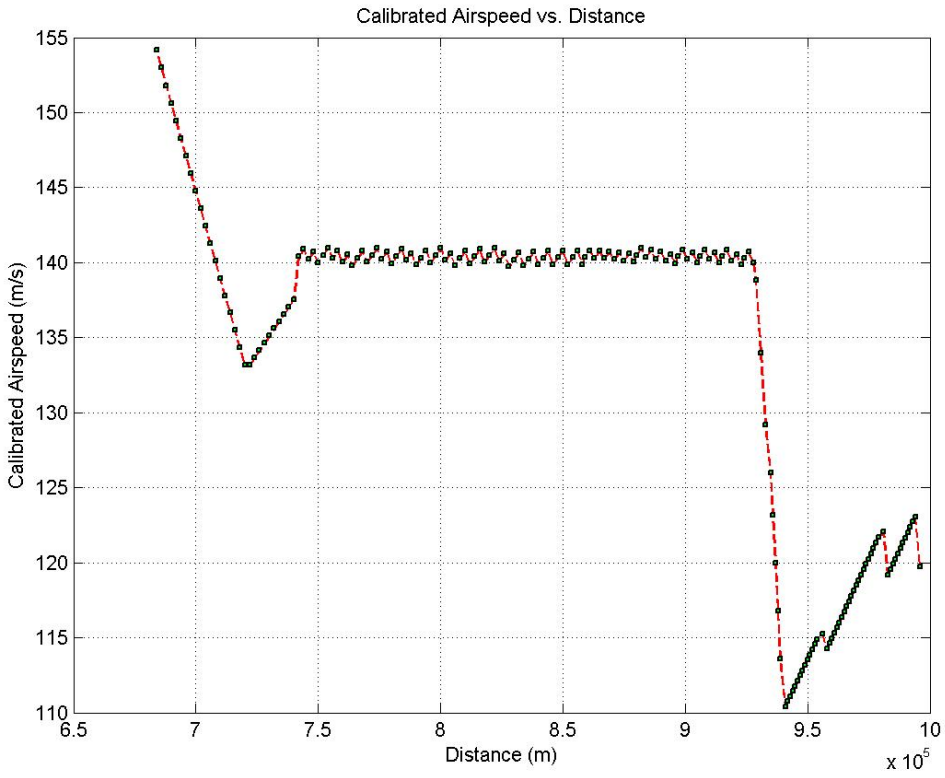

Figure 5.3: Restricted Descent Phase: V_{CAS} vs. Distance.

Comparing the above restricted descent with an unrestricted CDA trajectory (Figure 5.4) provided potentially significant results. It is worth noting that each descent is part of a complete trajectory, so the results compare each descent starting from the same horizontal distance to the goal. During descent the restricted approach consumed

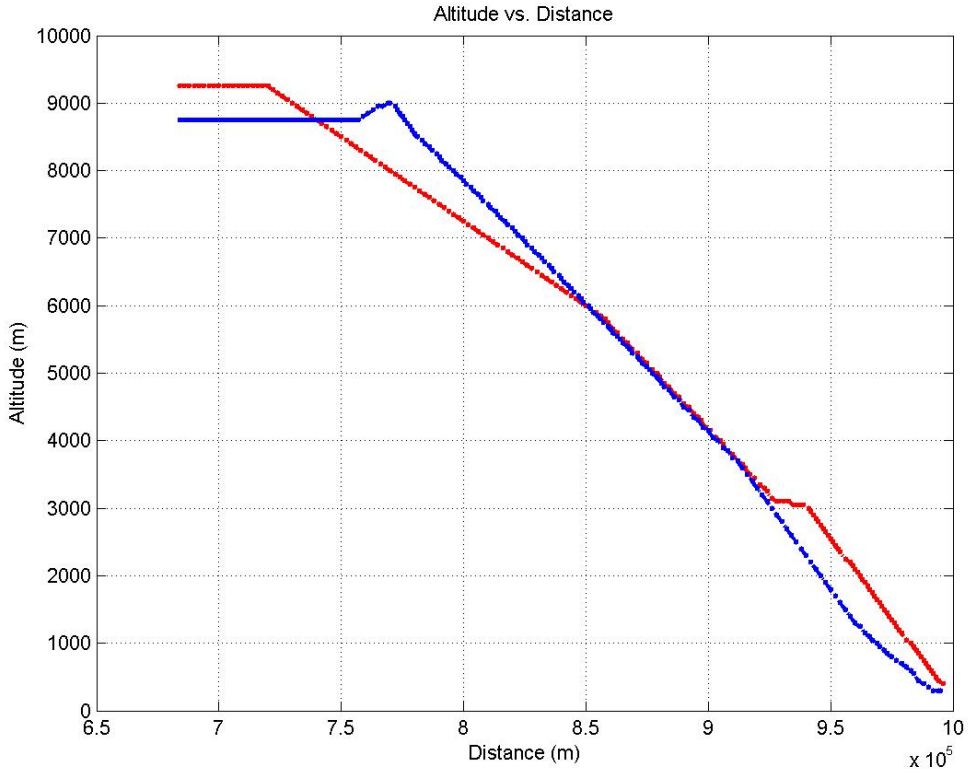

Figure 5.4: Restricted (Red) vs. Unrestricted (Blue) Descent Phase: Altitude vs. Distance.

272.2 kg of fuel while the CDA consumed 252.9 kg, demonstrating a 7.1% improvement in fuel efficiency. Additionally, comparing the restricted approach to CDA reduced the the descent time from 29.6 minutes to 25.2 minutes (up to the landing approach). While these numbers represent significant improvements in efficiency, both in flight time and fuel consumption, they only cover one phase of an entire trajectory. In order to determine the true significance of these results, complete vertical trajectories must also be studied.

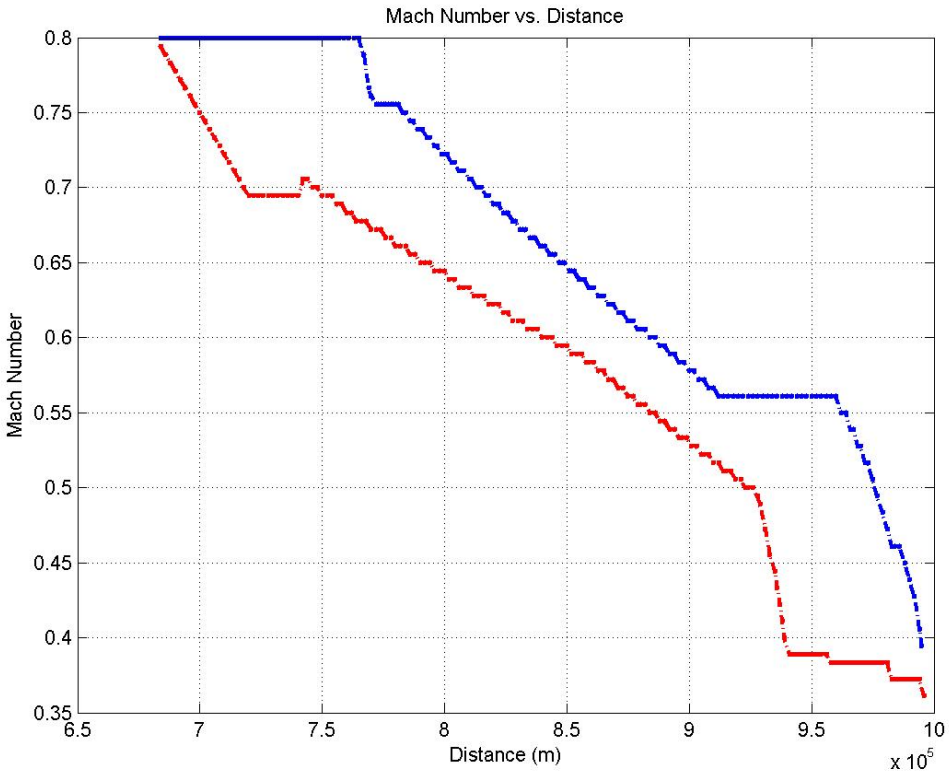

Figure 5.5: Restricted (Red) vs. Unrestricted (Blue) Descent Phase: Mach Number vs. Distance.

5.3 Complete Vertical Profile Analysis

The descent phase results discussed in Section 5.2 form only part of the complete analysis of vertical trajectories. As mentioned in the previous section, those results were simply the descent portions of complete trajectory simulations. The analysis of the previous section was included primarily to emphasize discrete search algorithms' ability to handle constraints, but was also included because typically such analyses are completed for each flight phase separately due to the difficulty of modeling constraints in complete trajectories.

This thesis' trajectory optimization algorithm can be easily extended to simulate

complete vertical trajectories without separating the climb, cruise, and descent phases. Under the exact same conditions described for the descent phase results (Section 5.2), the same efficiency comparison will be provided for complete vertical trajectories. Figures 5.6 and 5.7 compare altitude and Mach number respectively vs. horizontal distance for restricted and unrestricted trajectories.

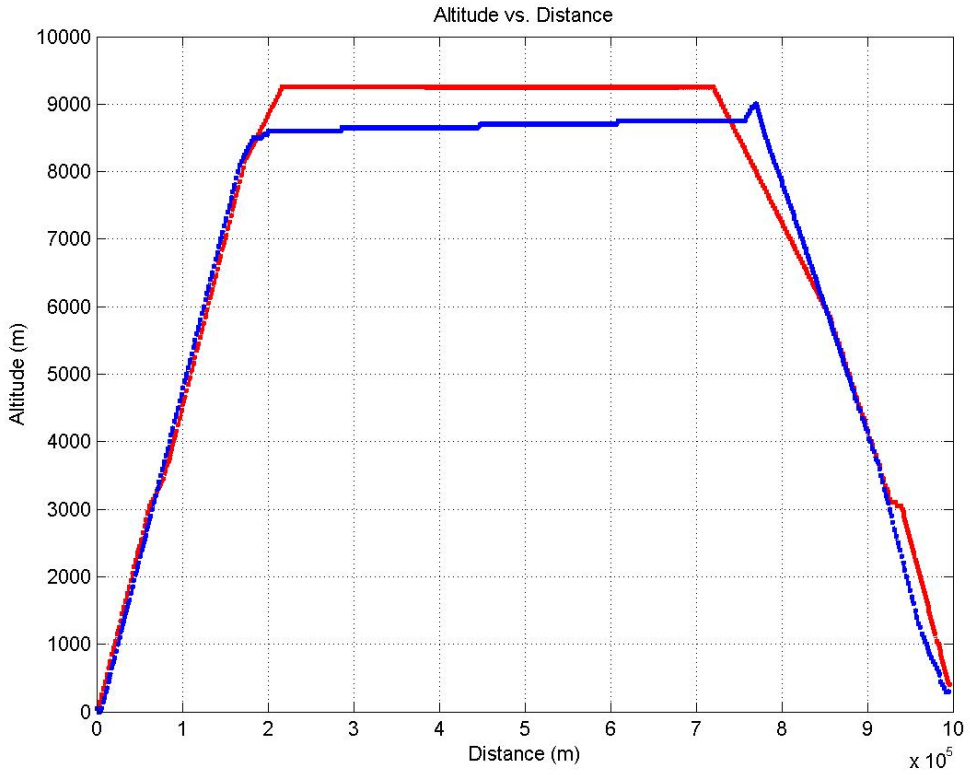

Figure 5.6: Restricted (red) vs. unrestricted (blue) complete trajectory: altitude vs. distance.

Given complete vertical trajectories, additional comparisons can be discussed for the climb and cruise phases. In Figure 5.6 a short decrease in flight path angle (γ) occurs in the restricted trajectory just above 10,000 ft as the aircraft moves above the 250 knot Calibrated Airspeed limit. This short segment allows the aircraft to accelerate quickly before continuing its climb. Comparing the cruise phase, one can see the restricted

aircraft flying at constant altitude while the unrestricted one follows a more efficient step climb (in a continuous algorithm this would be a continuous gradual climb, but limitations of discrete methods result in small step climbs).

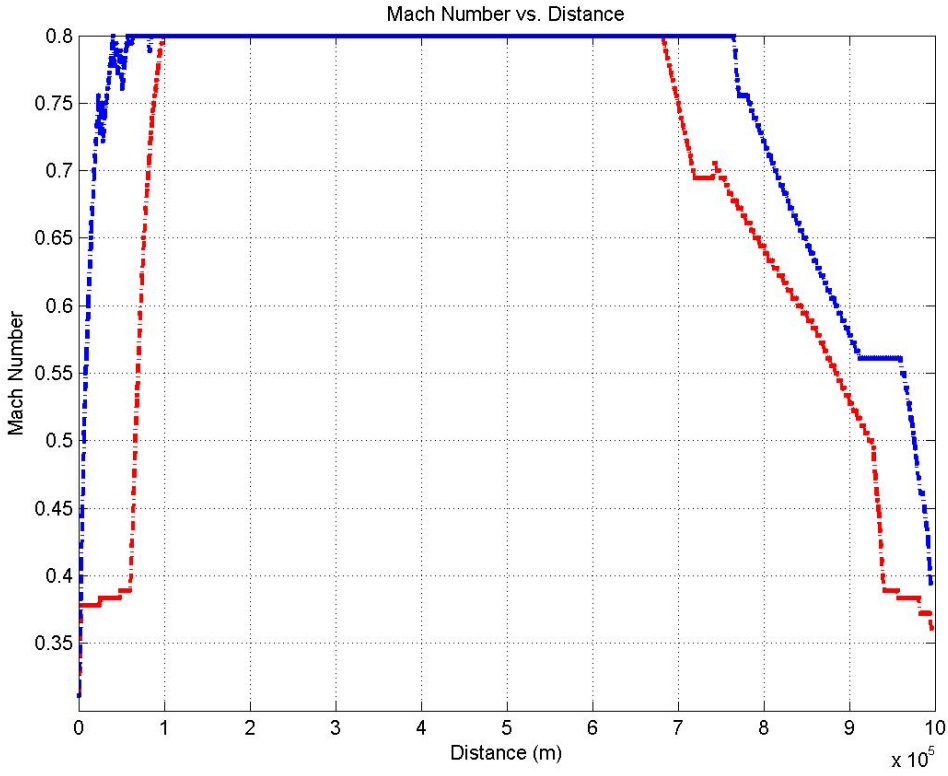

Figure 5.7: Restricted (red) vs. unrestricted (blue) complete trajectory: Mach number vs. distance.

Both trajectories compared in this section represent a relatively short flight of 1000 *km* total horizontal distance, and again are under the same conditions as the descent analysis. The unrestricted flight resulted in the consumption of 2472 kg of fuel and a total flight time of 80.5 minutes, while the unrestricted flight consumed 2260 kg of fuel in a flight time of 72 minutes. This resulted in a fuel savings of 8.6% and over an 8.5 minute reduction in flight time (almost 11%), demonstrating that removing unnecessary ATC restrictions on all phases of commercial flight can have a significant combined effect

on efficiency.

Chapter 6

Horizontal Trajectory Analysis

The results discussed in Chapter 5 compared current ATC procedures with more efficient procedures that may be possible with the implementation of the NextGen system. Unlike the vertical trajectory results, this chapter will compare two future horizontal trajectory schemes that are both improvements to the current procedures. This chapter will first describe the proposed lateral route planning methods and what they would require from the ATC system in order to be feasible. Then a statistical analysis comparing the two methods in the presence of varying winds will be presented.

6.1 NextGen Lateral Route Planning

Section 2.2.1 introduced horizontal trajectory procedures currently used by the ATC system. Lateral flight planning and navigation use a system of waypoints located at pre-defined coordinates accross the U.S. airspace. At high altitudes these are typically separated by 100 to 200 km or more depending on the region, resulting in a flight time on the order of 10 minutes or more between waypoints.

NextGen's proposed improvements to lateral route planning include implementing Trajectory Based Operations (TBO), which was briefly introduced in Section 5.1. The use of TBO would allow an aircraft to be cleared to fly a three-dimensional tube of airspace rather than the current waypoint method which only clears aircraft to fly directly between wayopints at constant altitude. This would result in a limited but useful amount of freedom to an aircraft's trajectory and ultimately provide the potential

to improve the overall efficiency of the ATC system.

The two horizontal trajectory schemes that were used to obtain this chapter's results are both based on the idea of optimally selecting the location of a trajectory's waypoints. Future improvements to the ATC system, such as TBO, would allow each flight to follow a unique series of waypoints without impeding on ATC safety. How the two methods differ is by the allowed distance between waypoints. The first scheme more closely resembles current lateral route procedures; its waypoint locations are optimally selected for predicted wind patterns, but they maintain the larger waypoint separations currently in use. The second scheme represents a discrete approximation of a continuous lateral route. The minimum distance between waypoints is greatly reduced, so waypoints may only be separated by one minute or less of cruise flight time. Maximum distance between waypoints remains the same as the first scheme, meaning both may return the same optimal route under certain conditions, but the second has the ability to more finely tune the route.

In a future ATC system where TBO became the norm for lateral route procedures, both of the above trajectory schemes would be feasible from a controller perspective. However, this does not mean that each would have equal costs to implement. Trajectories with small waypoint separations, or even continuous trajectories, would require more effort to navigate accurately. While both methods would be feasible, the near-continuous lateral trajectories would require various aircraft on-board software and controller tools to be redesigned for compatibility. Keeping procedures closer to the current system will make future transitions smoother, so the key is to weigh the cost of implementing a new method against the efficiency improvements it may provide. The following comparison will seek to determine if finely optimizing lateral routes for wind will provide enough efficiency improvement to justify the additional effort required to use such routes.

6.2 Statistical Wind Analysis

The results provided in this section are based on a 31-day wind sample from January, 2010 (Appendix B). A pair of simulations were completed for each wind model which compare routes with typical waypoint separations against ones that allow much smaller

separations. Each simulation represents a flight from the Dallas/Fort-Worth International Airport to the Minneapolis/St. Paul International Airport, approximately a 1500 km flight.

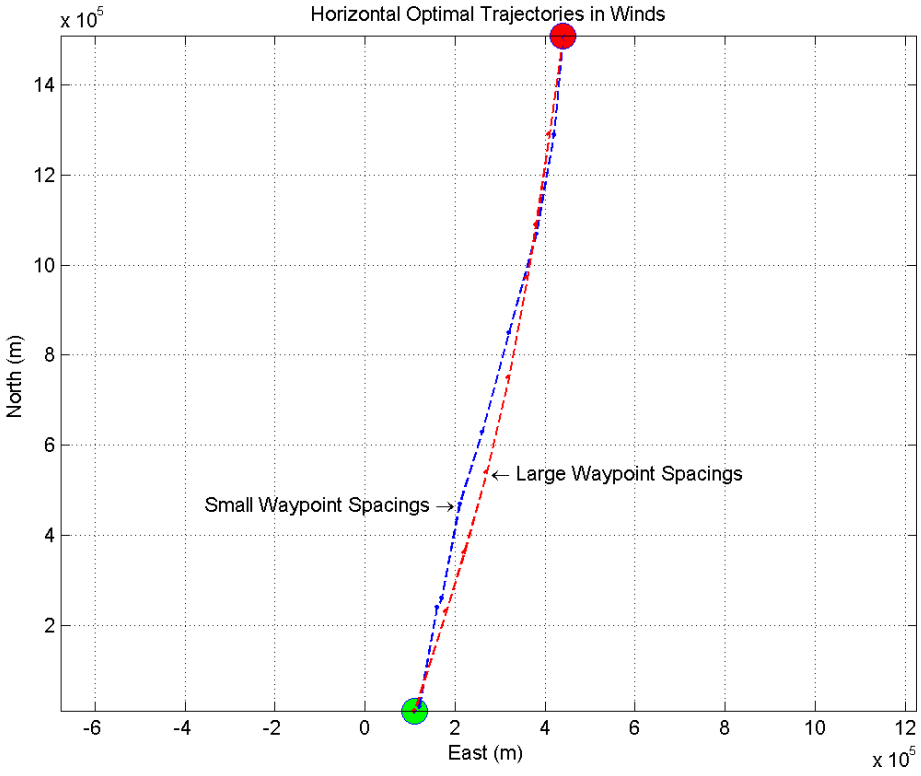

Figure 6.1: Horizontal Trajectory Comparison: Jan. 9, 2010 Wind Data

This chapter's results use the Boeing 777-300 aircraft model as described in Section 3.3.2. Trajectories represent the cruise phase of commercial flight which are generally flown at constant altitude and Mach number. Typical cruise altitude and Mach number for a Boeing 777-300 were used to produce the results.

$$M_{cruise} = 0.84 \tag{6.1}$$

$$h_{cruise} = 11,000\ m \tag{6.2}$$

Since the trajectories were flown at constant Mach and altitude, optimizing for time or fuel results in the same trajectory.

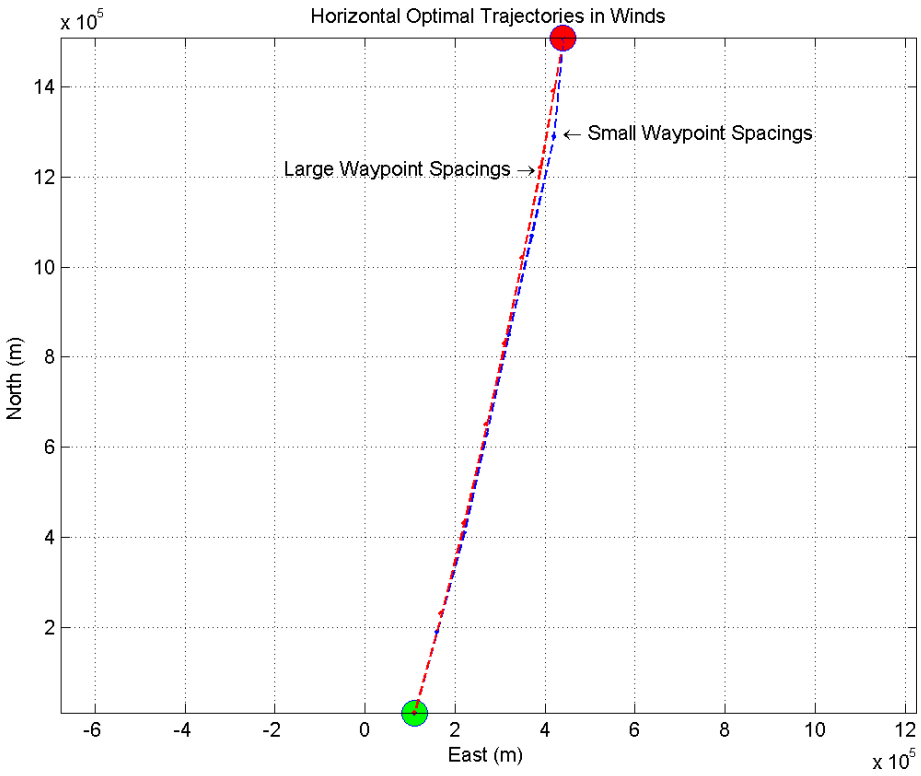

Figure 6.2: Horizontal Trajectory Comparison: Jan. 15, 2010 Wind Data

A grid comprised of 78 x and 152 y divisions was used along with the following grid spacings:

$$\Delta x = \Delta y = 10000\ m \tag{6.3}$$

Both lateral route schemes used the same maximum search depth, while the scheme that forced larger waypoint separations also used a minimum search depth.

$$N_{d_{max}} = 22 \tag{6.4}$$

$$N_{d_{min}} = 10 \tag{6.5}$$

The combination of the above search depths and grid spacing result in typical separation distances between waypoints for high altitude route planning as discussed in Section 6.1 (when using both minimum and maximum search depth, $N_{d_{min}}$ and $N_{d_{max}}$ respectively). When both the minimum and maximum search depths are enforced the distance between waypoints is restricted to approximately 100 to 200 km.

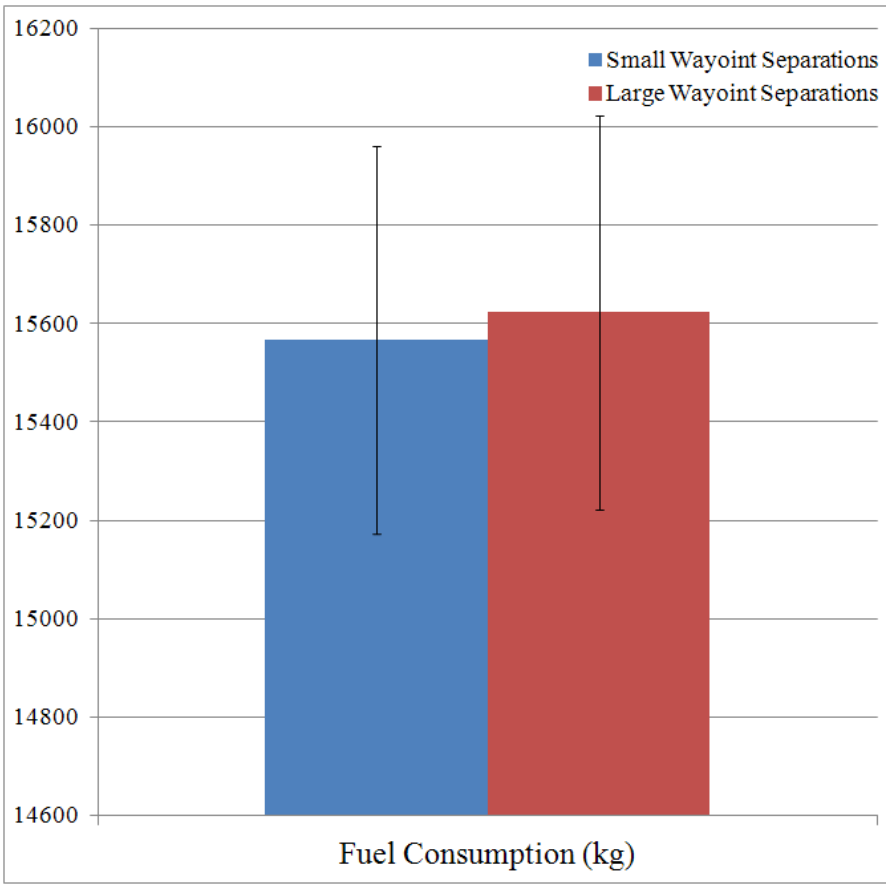

Figure 6.3: Horizontal Trajectory Comparison Results: Fuel Averages and Standard Deviations

The following will describe the results of comparing both the above discussed optimal waypoint lateral route schemes. Both methods represent improvements to the current system, so the analysis will be to determine if there is any benefit from implementing the higher-cost procedure in future ATC systems. One noticeable observation of the 31 data

sets was that simulations that allowed small waypoint separations often selected larger spacings. In fact, several sets of comparisons resulted in almost identical trajectories and waypoint locations. A sample of this is provided in Figure 6.2. While some comparisons resulted in larger differences in route structure, as demonstrated in Figure 6.1, trajectories generally had small differences between the two waypoint schemes.

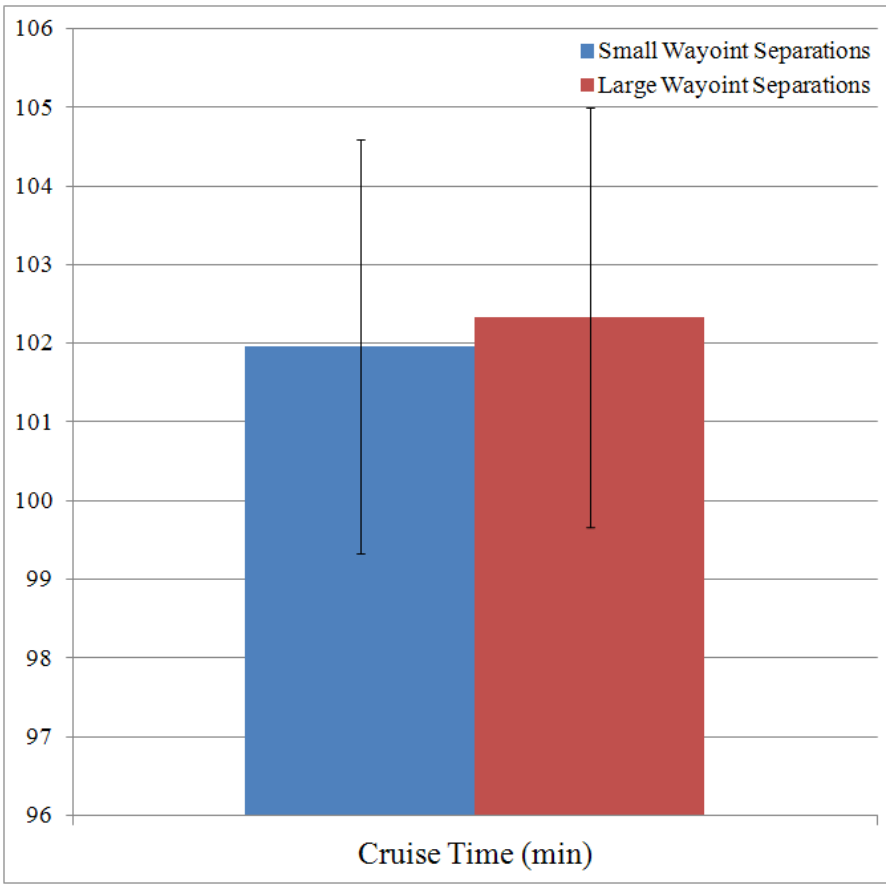

Figure 6.4: Horizontal Trajectory Comparison Results: Time Averages and Standard Deviations

These visual observations were reinforced by the statistical analysis of these results. The average fuel consumption for the larger waypoint separation trajectories was 15,623 kg with a standard deviation of 400 kg, while the trajectories that allowed smaller separations consumed on average 15,567 kg of fuel with a standard deviation of 394 kg

(Figure 6.3). This results in no statistical improvement in fuel consumption.

Comparing flight times between the two waypoint methods showed results similar to those of fuel consumption, as can be seen in Figure 6.4. Average flight time for larger waypoint separations was 102.33 minutes with a standard deviation of 2.66 minutes, and with smaller separation distances the average was 101.96 minutes with a standard deviation of 2.62 minutes. This again demonstrates that no statistically significant improvements are observed when smaller waypoint separations are allowed for cruise trajectories.

Chapter 7

Conclusions and Discussion

This thesis provides two key contributions: the formulation of a trajectory optimization algorithm using discrete search methods and the study of vertical and horizontal commercial flight trajectories using the provided algorithm. Commercial aircraft trajectory optimization research, especially for the vertical profile, is typically conducted using continuous optimization algorithms. The discrete search strategy provides a unique opportunity to study heavily constrained aircraft trajectories in order to determine the potential benefits of removing overly-restrictive ATC constraints from future ATC systems.

The discrete search trajectory optimization algorithm provided in Chapter 4 was able to easily model numerous constraints for vertical and horizontal flight profiles. Complex ATC procedures such as the segmented flight structure of vertical trajectories were demonstrated in Chapter 5. Additionally, the horizontal algorithm was used to model a lateral route defined by optimally selected waypoints of various separation distances. This algorithm was presented in a way that it could easily be extended to simulate 4D trajectories (three physical search dimensions plus airspeed).

Vertical trajectory results provided in Chapter 5 discussed the potential benefit of removing unnecessary ATC restrictions from vertical flight procedures. The chapter first discussed the feasibility of removing certain ATC restrictions from vertical trajectories in future ATC systems. A comparison of restricted and unrestricted trajectories was then presented for both the descent phase and complete vertical trajectories. The results demonstrated fuel efficiency improvements of 7.1% for the descent phase and 8.6% for

the entire trajectory. Additionally, flight times were reduced from 29.6 to 25.2 minutes in descent. and 80.5 to 72 minutes overall. These represent significant savings given the current state of the commercial flight industry. However, the results were obtained for a single, relatively short flight, so the results do not carry much statistical weight. Chapter 8 discusses possible future work in this area to obtain statistically significant results.

The horizontal results provided in Chapter 6 take a different approach than the vertical results did. Instead of comparing current ATC procedures to possible future implementations, the chapter presented two potential future lateral route planning schemes. Both optimally selected the locations of waypoints in the presence of wind, but one allowed much smaller separations between consecutive waypoints while the other used larger separations typical of current high altitude cruise flights. The purpose of this comparison was to analyze the benefit of using near continuous lateral routes knowing that the cost of implementing such a scheme in future ATC systems would be greater. The results included 31 sets of comparisons between the two waypoint schemes representing wind models from the 31 days of January, 2010. A statistical analysis concluded that no statistically significant efficiency improvements in either fuel consumption or flight time were demonstrated. This means that in future ATC systems it would be desirable to implement lateral route procedures similar to current methods while introducing the optimal selection of waypoint coordinates.

Chapter 8

Recommendations for Future Research

The trajectory optimization algorithm and results provided in this paper lay the foundation for a variety of additional studies within the realm of commercial aircraft trajectory optimization. There are numerous extensions to the vertical and horizontal trajectory studies which continue the analyses presented in this paper. Additionally, extending this paper's algorithm into a 4D trajectory optimization algorithm (three physical search dimensions in addition to a speed dimension) could allow for a more detailed analysis. Some extensions may be studied with any trajectory profile: the affect of varying take-off weight on efficiency, testing different aircraft types, and varying the performance index.

8.1 Further Vertical Trajectory Analysis

The vertical profile results presented in this paper provide a basis to expand from. An analysis of different flight lengths would provide a more effective study of the efficiency improvements possible by removing unnecessary ATC restrictions. Additionally, an analysis in the presence of varying wind models would be necessary to obtain statistically significant results for the vertical profile.

Aside from efficiency analyses, other opportunities for studying vertical trajectories exist. It has been proven that the most fuel efficient cruise trajectory follows a periodic

pattern[25]. This paper's vertical algorithm produces periodic behavior during cruise when $c_t = 0$. Since the focus of this paper is to determine the potential benefits of removing certain ATC procedures, little time was spent studying this arguably surprising result (see Figure 8.1). When the cost index is defined to purely optimize for fuel consumption, the periodic characteristics appear. Despite being the most fuel efficient path to fly, this trajectory would not be feasible or practical for commercial flight due to the loss of passenger comfort and increase in flight time from the additional distance traveled, thus it would be a purely academic study.

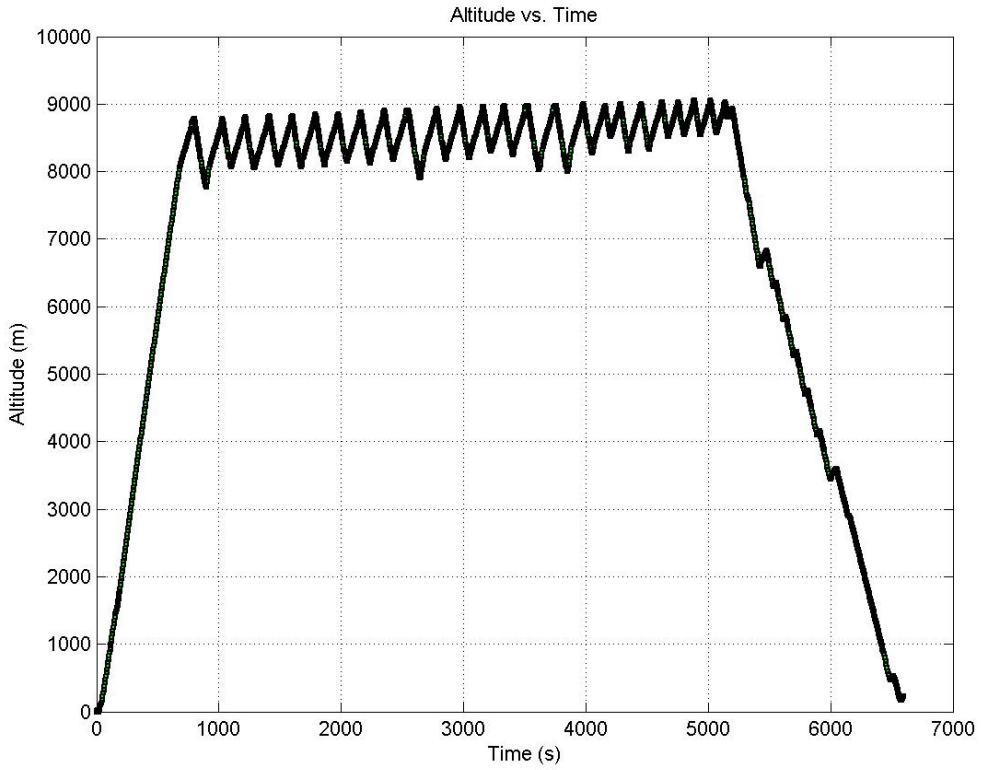

Figure 8.1: Periodic flight resulting from optimizing purely to minimize fuel consumption.

A final area of study for vertical trajectories is possibly related to the periodic minimum fuel result. One characteristic of this paper's unrestricted vertical trajectories

is a slight climb noticeable just before the descent phase (Figure 8.2). This characteristic becomes more noticeable as the trajectory optimizes more for fuel consumption. Further study of this characteristic to determine its cause would provide an interesting analysis.

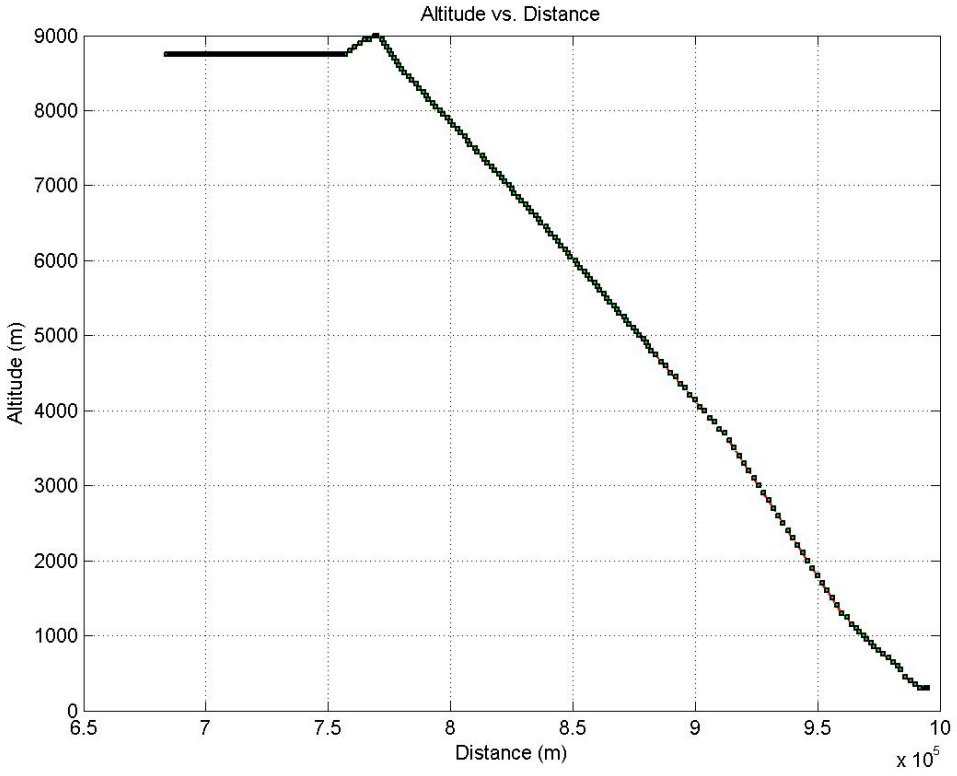

Figure 8.2: Figure of slight climb before descent.

8.2 Further Horizontal Trajectory Analysis

The results discussed in Chapter 6 provide a comparison of possible future improvements to lateral route planning procedures, but an additional comparison to the current airway system would be a useful analysis. The current airway structure uses predefined waypoint coordinates which are typically separated by 50 to over 100 miles at high

altitudes. This does not allow for the level of optimization possible with the methods discussed in Chapter 6. Studies evaluating the potential benefits of moving to one of the more optimal lateral route procedures would prove useful in determining if the efficiency improvements would be significant enough to justify the cost of implementing new lateral navigation procedures.

8.3 4D Trajectory Analysis

As technology continues to progress, planing trajectories without separating the vertical and horizontal components will become more feasible. The key issues presented by 4D trajectory planning results from the limitations of optimization methods. While the discrete search trajectory algorithm presented in this paper can easily be extended to 4D search (three physical dimensions and speed), memory and runtime issues may greatly limit the accuracy such a method could achieve. Additionally, continuous parameter optimization methods are able to more efficiently simulate trajectories with three physical dimensions, but this becomes more difficult when modeling ATC constraints and procedures. A study in the area of 4D trajectories may compare the efficiency and accuracy of different optimization methods in addition to analyzing the trade-off between efficiency and accuracy for various settings of individual algorithms.

References

[1] Joint Planning and Development Office. Next Generation Air Transportation System: Integrated Plan. *http://www.jpdo.gov/library/NGATS_v1_1204r.pdf*, 2004.

[2] N. R. Zagalsky, R. E. Irons, and R. L. Schultz. The Energy State Approximation and Minimum-Fuel Fixed-Range Trajectories. *Journal of Aircraft*, (Vol. 8, No. 8), 1971.

[3] R. L. Schultz and N. R. Zagalsky. Aircraft Performance Optimization. *Journal of Aircraft*, (Vol. 9, No. 2, Feb.):108–114, 1972.

[4] J. F. Barman and H. Erzberger. Fixed-Range Optimal Trajectories for Short Haul Aircraft. *Journal of Aircraft*, (Vol. 13, No. 10):748–754, 1976.

[5] A. J. Calise. Extended Energy Management Methods for Flight Performance Optimization. *AIAA Journal*, (Vol. 15, No. 3):314–321, 1977.

[6] H. Erzberger and H. Lee. Constrained Optimum Trajectories with Specified Range. *Journal of Guidance, Control and Dynamics*, (Vol. 3, No. 1):78–85, 1980.

[7] J. W. Burroughs. Fuel-Optimal Aircraft Trajectories with Fixed Arrival Times. *Journal of Guidance and Control*, (Vol. 6, No. 1, Jan.-Feb.):14–19, 1983.

[8] A. J. Calise. Singular Perturbation Techniques for On-line Optimal Flight-Path Control. *Journal of Guidance and Control*, (Vol. 3, No. 4):398–405, 1981.

[9] D. P. Price, J. C. Calise, and D. D. Moerder. Piloted Simulation of an Onboard Trajectory Optimization Algorithm. *Journal of Guidance and Control*, (Vol. 7, No. 3):355–360, 1984.

[10] A. Chakravarty. Four-Dimensional Fuel-Optimal Guidance in the Presence of Winds. *Journal of Guidance, Control and Dynamics*, (Vol. 8, No. 1, Jan.-Feb.):16–22, 1985.

[11] R. L. Schultz. Three-Dimensional Trajectory Optimization for Aircraft. *Journal of Guidance, Control and Dynamics*, (Vol. 13, No. 6, Nov.-Dec.):936–943, 1990.

[12] J. A. Sorenson and M. H. Waters. Generation of Optimum Vertical Profiles for an Advanced Flight Management System. *NASA CP-165674*, March 1981.

[13] G. Menga and H. Erzberger. Time-Controlled Descent Guidance in Uncertain Winds. *Journal of Aircraft*, (Vol. 1, No. 2, March-April), 1978.

[14] H. Erzberger. Automation of On-Board Flightpath Management. *NASA TM 84212*, December 1981.

[15] R. L. Schultz and D. A. Shaner. *U. S. Patent No. 6,266,610 B1*, Washington, DC: U.S. Patent and Trademark Office.

[16] R. A. Slattery and Y. J. Zhao. Trajectory Synthesis for Air Traffic Automation. *Journal of Guidance, Control and Dynamics*, (Vol. 20, No. 2,March-April):232–238, 1997.

[17] F. J. Hale. Introduction to Aircraft Performance, Selection, and Design. *John Wiley & Sons*, (Sections 4-2 to 4-5, Chap. 10), 1984.

[18] N. X. Vinh. Flight Mechanics of High-Performance Aircraft. *Cambridge University Press*, (Chap. 2, Sec. 4.4, Appendix 2), 1993.

[19] D. G. Hull. Fundamentals of Airplane Flight Mechanics. *Springer*, (Section 3.8), 2007.

[20] Jr. Anderson, J. D. Aircraft Performance and Design. (Chapters 3, 5), 1999.

[21] M. R. Jackson, Y. J. Zhao, and R. A. Slattery. Sensitivities of Trajectory Prediction in Air Traffic Management. *Journal of Guidance, Control and Dynamics*, (Vol. 22, No. 2, March-April):219–228, 1998.

[22] D. Wu and Y. J. Zhao. Performances and Sensitivities of Optimal Trajectory Generation for Air Traffic Control Automation. *AIAA*, (August):1–22, 2009.

[23] The Boeing Company. Technical Characteristics - Boeing 777-300. *http://www.boeing.com/commercial/777family/pf/pf_300product.html*, 2011.

[24] M. R. Jardin and A. E. Bryson Jr. Neighboring Optimal Aircraft Guidance in Winds. *Journal of Guidance, Control and Dynamics*, (Vol. 24, No. 4, Jul.-Aug.):710–715, 2001.

[25] J. L. Speyer. Periodic Optimal Flight. *Journal of Guidance, Control and Dynamics*, (Vol. 19, No. 4, July):745–755, 1996.

Appendix A

Nomenclature

Table A.1: Nomenclature

Variable	Definition
a	Speed of sound
(C_D, C_L)	(Drag, lift) coefficient
C_{D_0}	Parasite drag coefficient
c_f	Fuel weight coefficient for cost funtion
c_t	Time weight coefficient for cost funtion
D	Drag force
g	Acceleration of gravity
h	Geometric altitude
h_p	Pressure altitude
I	Performance index or cost function
K	Induced drag factor
l_a	Temperature lapse rate in standard atmosphere
L	Lift force
m	Aircraft mass
m_f	Mass of fuel consumed
M	Mach number

Continued on next page

Table A.1 – continued from previous page

Acronym	Meaning
p	Pressure
R	Specific gas constant
s	Horizontal flight distance
S	Wing platform area
T	Engine thrust
t	Time
V	Airspeed
V_{CAS}	Calibrated airspeed
W_0	Take-off weight
(W_x, W_y)	(Eastward, Northward) wind component
W_h	Vertical wind component
(W_V, W_Ψ, W_γ)	(Airspeed, heading, pitch) wind component
(x, y)	(East, North) coordinate
γ	Air-relative flight path angle
Θ	Air temperature
ϕ	aircraft bank angle
ρ	Air density
Ψ	Air-relative heading angle
$(\ )_{SLS}$	Sea level standard value
$(\ )_{ISA}$	International standard atmosphere
$(\ )_T$	Value at tropopause

Appendix B

Wind Polynomials

The following polynomials represent wind data for the 31 days of January 2010. Wind data was provided by the National Operational Model Archive & Distribution System (NOAA), and the polynomials were created by fitting the data using 5th-order polynomials. The polynomials are functions of latitude (x) and longitude (y) in units of degrees, and are presented in pairs representing East and North components of wind in meters per second.

$$\begin{aligned} W_{x_{Day1}} &= 0.00011269 \cdot x^4 + 8.9543 \cdot 10^{-5} \cdot x^3 \cdot y - 3.0564 \cdot 10^{-5} \cdot x^2 \cdot y^2 \\ &\quad +8.209 \cdot 10^{-6} \cdot x \cdot y^3 - 1.575 \cdot 10^{-6} \cdot y^4 - 0.0070988 \cdot x^3 - 0.018027 \cdot x^2 \cdot y \\ &\quad +0.0049933 \cdot x \cdot y^2 - 0.0011637 \cdot y^3 - 0.72046 \cdot x^2 + 1.2419 \cdot x \cdot y \\ &\quad -0.30732 \cdot y^2 + 67.5502 \cdot x - 38.6178 \cdot y - 1668.0805 \end{aligned} \tag{B.1}$$

$$\begin{aligned} W_{y_{Day1}} &= 2.6349 \cdot 10^{-6} \cdot x^4 + 4.0861 \cdot 10^{-5} \cdot x^3 \cdot y - 2.3707 \cdot 10^{-5} \cdot x^2 \cdot y^2 \\ &\quad -7.9507 \cdot 10^{-6} \cdot x \cdot y^3 - 1.0105 \cdot 10^{-5} \cdot y^4 + 0.0046428 \cdot x^3 - 0.0091442 \cdot x^2 \cdot y \\ &\quad +0.00077262 \cdot x \cdot y^2 - 0.0043858 \cdot y^3 - 0.764 \cdot x^2 + 0.55866 \cdot x \cdot y - 0.78006 \cdot y^2 \\ &\quad +42.835 \cdot x - 66.2848 \cdot y - 2215.7012 \end{aligned} \tag{B.2}$$

$$W_{x_{Day2}} = 5.3831 \cdot 10^{-5} \cdot x^4 + 0.0001009 \cdot x^3 \cdot y - 1.6494 \cdot 10^{-5} \cdot x^2 \cdot y^2$$

$$+3.1005 \cdot 10^{-5} \cdot x \cdot y^3 + 8.5122 \cdot 10^{-6} \cdot y^4 + 0.0042753 \cdot x^3 - 0.016428 \cdot x^2 \cdot y$$
$$+0.010311 \cdot x \cdot y^2 + 0.0018829 \cdot y^3 - 1.3389 \cdot x^2 + 1.6386 \cdot x \cdot y + 0.028556 \cdot y^2$$
$$+93.4586 \cdot x - 22.0239 \cdot y - 1479.4869 \quad \text{(B.3)}$$

$$W_{y_{Day2}} = -2.2373 \cdot 10^{-5} \cdot x^4 + 2.7454 \cdot 10^{-5} \cdot x^3 \cdot y - 6.0653 \cdot 10^{-5} \cdot x^2 \cdot y^2$$
$$-3.2719 \cdot 10^{-5} \cdot x \cdot y^3 - 2.6033 \cdot 10^{-5} \cdot y^4 + 0.0071674 \cdot x^3 - 0.014991 \cdot x^2 \cdot y$$
$$-0.0034609 \cdot x \cdot y^2 - 0.0085943 \cdot y^3 - 1.1741 \cdot x^2 + 0.39553 \cdot x \cdot y - 1.134 \cdot y^2$$
$$+47.5853 \cdot x - 74.5706 \cdot y - 2137.8674 \quad \text{(B.4)}$$

$$W_{x_{Day3}} = 1.7235 \cdot 10^{-5} \cdot x^4 + 0.00012983 \cdot x^3 \cdot y + 1.9062 \cdot 10^{-5} \cdot x^2 \cdot y^2$$
$$+1.177 \cdot 10^{-5} \cdot x \cdot y^3 + 6.151 \cdot 10^{-7} \cdot y^4 + 0.013666 \cdot x^3 - 0.012613 \cdot x^2 \cdot y$$
$$+0.0019461 \cdot x \cdot y^2 - 0.00032066 \cdot y^3 - 1.7118 \cdot x^2 + 0.66919 \cdot x \cdot y - 0.10625 \cdot y^2$$
$$+70.5925 \cdot x - 16.2998 \cdot y - 1049.5496 \quad \text{(B.5)}$$

$$W_{y_{Day3}} = -6.0021 \cdot 10^{-5} \cdot x^4 + 4.0346 \cdot 10^{-5} \cdot x^3 \cdot y - 1.6956 \cdot 10^{-5} \cdot x^2 \cdot y^2$$
$$+2.3955 \cdot 10^{-6} \cdot x \cdot y^3 - 7.254 \cdot 10^{-7} \cdot y^4 + 0.014345 \cdot x^3 - 0.0079105 \cdot x^2 \cdot y$$
$$+0.0023533 \cdot x \cdot y^2 - 0.00043091 \cdot y^3 - 1.2366 \cdot x^2 + 0.55673 \cdot x \cdot y - 0.11299 \cdot y^2$$
$$+49.0569 \cdot x - 13.9796 \cdot y - 736.7743 \quad \text{(B.6)}$$

$$W_{x_{Day4}} = -9.342 \cdot 10^{-5} \cdot x^4 + 0.00014465 \cdot x^3 \cdot y - 2.7969 \cdot 10^{-5} \cdot x^2 \cdot y^2$$
$$-5.7793 \cdot 10^{-7} \cdot x \cdot y^3 - 4.7129 \cdot 10^{-7} \cdot y^4 + 0.032587 \cdot x^3 - 0.023413 \cdot x^2 \cdot y$$
$$+0.002379 \cdot x \cdot y^2 - 3.7947 \cdot 10^{-5} \cdot y^3 - 3.2744 \cdot x^2 + 1.167 \cdot x \cdot y$$
$$-0.04161 \cdot y^2 + 124.3577 \cdot x - 16.6891 \cdot y - 1486.088 \quad \text{(B.7)}$$

$$W_{y_{Day4}} = -9.1871 \cdot 10^{-5} \cdot x^4 + 6.1267 \cdot 10^{-5} \cdot x^3 \cdot y - 3.0809 \cdot 10^{-5} \cdot x^2 \cdot y^2$$
$$-2.0155 \cdot 10^{-6} \cdot x \cdot y^3 - 2.682 \cdot 10^{-6} \cdot y^4 + 0.021342 \cdot x^3 - 0.013692 \cdot x^2 \cdot y$$
$$+0.0017771 \cdot x \cdot y^2 - 0.0011654 \cdot y^3 - 1.9376 \cdot x^2 + 0.7125 \cdot x \cdot y$$
$$-0.21957 \cdot y^2 + 71.6126 \cdot x - 22.9972 \cdot y - 1153.6549 \quad \text{(B.8)}$$

$$
\begin{aligned}
W_{x_{Day5}} &= -0.0002039 \cdot x^4 + 0.00014983 \cdot x^3 \cdot y - 5.392 \cdot 10^{-5} \cdot x^2 \cdot y^2 \\
&\quad +7.787 \cdot 10^{-6} \cdot x \cdot y^3 + 2.321 \cdot 10^{-6} \cdot y^4 + 0.049597 \cdot x^3 - 0.02827 \cdot x^2 \cdot y \\
&\quad +0.007106 \cdot x \cdot y^2 + 0.00065066 \cdot y^3 - 4.3772 \cdot x^2 + 1.8004 \cdot x \cdot y \\
&\quad -0.051243 \cdot y^2 + 168.1749 \cdot x - 26.5123 \cdot y - 2110.45 \qquad \text{(B.9)}
\end{aligned}
$$

$$
\begin{aligned}
W_{y_{Day5}} &= -3.4564 \cdot 10^{-5} \cdot x^4 + 9.9522 \cdot 10^{-5} \cdot x^3 \cdot y - 7.1637 \cdot 10^{-5} \cdot x^2 \cdot y^2 \\
&\quad -3.5057 \cdot 10^{-5} \cdot x \cdot y^3 - 3.1182 \cdot 10^{-6} \cdot y^4 + 0.015559 \cdot x^3 - 0.025839 \cdot x^2 \cdot y \\
&\quad -0.0044826 \cdot x \cdot y^2 + 0.00018172 \cdot y^3 - 2.1522 \cdot x^2 + 0.59579 \cdot x \cdot y \\
&\quad +0.13617 \cdot y^2 + 73.6249 \cdot x + 4.0482 \cdot y - 462.0548 \qquad \text{(B.10)}
\end{aligned}
$$

$$
\begin{aligned}
W_{x_{Day6}} &= -0.0001579 \cdot x^4 + 0.0001664 \cdot x^3 \cdot y - 2.2833 \cdot 10^{-5} \cdot x^2 \cdot y^2 \\
&\quad +3.2546 \cdot 10^{-5} \cdot x \cdot y^3 + 3.7472 \cdot 10^{-6} \cdot y^4 + 0.043396 \cdot x^3 - 0.023895 \cdot x^2 \cdot y \\
&\quad +0.011716 \cdot x \cdot y^2 - 3.0927 \cdot 10^{-6} \cdot y^3 - 3.7947 \cdot x^2 + 2.0286 \cdot x \cdot y \\
&\quad -0.27297 \cdot y^2 + 159.3708 \cdot x - 45.4089 \cdot y - 2508.9065 \qquad \text{(B.11)}
\end{aligned}
$$

$$
\begin{aligned}
W_{y_{Day6}} &= -4.7401 \cdot 10^{-5} \cdot x^4 + 5.3755 \cdot 10^{-5} \cdot x^3 \cdot y - 0.00010024 \cdot x^2 \cdot y^2 \\
&\quad -2.6792 \cdot 10^{-5} \cdot x \cdot y^3 + 2.2576 \cdot 10^{-6} \cdot y^4 + 0.013049 \cdot x^3 - 0.025547 \cdot x^2 \cdot y \\
&\quad +0.00052494 \cdot x \cdot y^2 + 0.0018716 \cdot y^3 - 1.9544 \cdot x^2 + 1.0887 \cdot x \cdot y \\
&\quad +0.26367 \cdot y^2 + 83.7032 \cdot x + 4.1053 \cdot y - 595.5862 \qquad \text{(B.12)}
\end{aligned}
$$

$$
\begin{aligned}
W_{x_{Day7}} &= -8.9071 \cdot 10^{-7} \cdot x^4 + 0.00015935 \cdot x^3 \cdot y - 1.1917 \cdot 10^{-5} \cdot x^2 \cdot y^2 \\
&\quad +1.7819 \cdot 10^{-5} \cdot x \cdot y^3 + 2.9974 \cdot 10^{-6} \cdot y^4 + 0.018578 \cdot x^3 - 0.02074 \cdot x^2 \cdot y \\
&\quad +0.0065889 \cdot x \cdot y^2 + 0.00020629 \cdot y^3 - 2.2699 \cdot x^2 + 1.4086 \cdot x \cdot y \\
&\quad -0.15056 \cdot y^2 + 103.7742 \cdot x - 29.7762 \cdot y - 1645.8669 \qquad \text{(B.13)}
\end{aligned}
$$

$$
\begin{aligned}
W_{y_{Day7}} &= -4.5789 \cdot 10^{-5} \cdot x^4 + 5.3975 \cdot 10^{-5} \cdot x^3 \cdot y - 5.5463 \cdot 10^{-5} \cdot x^2 \cdot y^2 \\
&\quad -3.0265 \cdot 10^{-5} \cdot x \cdot y^3 + 2.2964 \cdot 10^{-6} \cdot y^4 + 0.012549 \cdot x^3 - 0.017236 \cdot x^2 \cdot y \\
&\quad -0.003256 \cdot x \cdot y^2 + 0.0022119 \cdot y^3 - 1.5392 \cdot x^2 + 0.47733 \cdot x \cdot y \\
&\quad +0.38705 \cdot y^2 + 56.3122 \cdot x + 18.1186 \cdot y - 86.9772 \qquad \text{(B.14)}
\end{aligned}
$$

$$
\begin{aligned}
W_{x_{Day8}} &= 0.00010879 \cdot x^4 + 9.4047 \cdot 10^{-5} \cdot x^3 \cdot y - 4.6914 \cdot 10^{-5} \cdot x^2 \cdot y^2 \\
&\quad +3.9896 \cdot 10^{-5} \cdot x \cdot y^3 - 5.0517 \cdot 10^{-6} \cdot y^4 - 0.0031075 \cdot x^3 - 0.020224 \cdot x^2 \cdot y \\
&\quad +0.015812 \cdot x \cdot y^2 - 0.004024 \cdot y^3 - 1.1286 \cdot x^2 + 2.3068 \cdot x \cdot y - 0.96608 \cdot y^2 \\
&\quad +108.532 \cdot x - 94.5697 \cdot y - 3295.2288 \qquad \text{(B.15)}
\end{aligned}
$$

$$
\begin{aligned}
W_{y_{Day8}} &= 2.7306 \cdot 10^{-6} \cdot x^4 + 2.8088 \cdot 10^{-5} \cdot x^3 \cdot y - 6.6188 \cdot 10^{-5} \cdot x^2 \cdot y^2 \\
&\quad +2.5881 \cdot 10^{-5} \cdot x \cdot y^3 + 7.9994 \cdot 10^{-6} \cdot y^4 + 0.0025704 \cdot x^3 - 0.016399 \cdot x^2 \cdot y \\
&\quad +0.01391 \cdot x \cdot y^2 + 0.0013975 \cdot y^3 - 0.94803 \cdot x^2 + 2.082 \cdot x \cdot y \\
&\quad -0.18805 \cdot y^2 + 92.3112 \cdot x - 46.6149 \cdot y - 2128.5583 \qquad \text{(B.16)}
\end{aligned}
$$

$$
\begin{aligned}
W_{x_{Day9}} &= 1.6985 \cdot 10^{-5} \cdot x^4 + 7.5352 \cdot 10^{-5} \cdot x^3 \cdot y - 3.3084 \cdot 10^{-5} \cdot x^2 \cdot y^2 \\
&\quad +3.174 \cdot 10^{-5} \cdot x \cdot y^3 - 1.0936 \cdot 10^{-5} \cdot y^4 + 0.011077 \cdot x^3 - 0.016273 \cdot x^2 \cdot y \\
&\quad +0.011877 \cdot x \cdot y^2 - 0.005721 \cdot y^3 - 1.8702 \cdot x^2 + 1.7793 \cdot x \cdot y \\
&\quad -1.0772 \cdot y^2 + 113.1757 \cdot x - 90.8901 \cdot y - 3169.8178 \qquad \text{(B.17)}
\end{aligned}
$$

$$
\begin{aligned}
W_{y_{Day9}} &= -1.2958 \cdot 10^{-5} \cdot x^4 + 5.3988 \cdot 10^{-5} \cdot x^3 \cdot y - 5.1251 \cdot 10^{-5} \cdot x^2 \cdot y^2 \\
&\quad +5.1986 \cdot 10^{-5} \cdot x \cdot y^3 - 2.3966 \cdot 10^{-5} \cdot y^4 + 0.0080931 \cdot x^3 - 0.017114 \cdot x^2 \cdot y \\
&\quad +0.020213 \cdot x \cdot y^2 - 0.011902 \cdot y^3 - 1.3715 \cdot x^2 + 2.7056 \cdot x \cdot y - 2.186 \cdot y^2 \\
&\quad +123.8915 \cdot x - 177.1158 \cdot y - 5372.7734 \qquad \text{(B.18)}
\end{aligned}
$$

$$
W_{x_{Day10}} = -3.9613 \cdot 10^{-5} \cdot x^4 + 0.00011592 \cdot x^3 \cdot y - 5.9197 \cdot 10^{-5} \cdot x^2 \cdot y^2
$$

$$+2.072 \cdot 10^{-6} \cdot x \cdot y^3 - 3.3726 \cdot 10^{-6} \cdot y^4 + 0.021553 \cdot x^3 - 0.026526 \cdot x^2 \cdot y$$
$$+0.0053159 \cdot x \cdot y^2 - 0.0013228 \cdot y^3 - 2.8133 \cdot x^2 + 1.5749 \cdot x \cdot y - 0.27339 \cdot y^2$$
$$+127.4632 \cdot x - 35.1916 \cdot y - 1929.7392 \quad \text{(B.19)}$$

$$W_{y_{Day10}} = 9.8349 \cdot 10^{-6} \cdot x^4 + 7.9499 \cdot 10^{-5} \cdot x^3 \cdot y - 3.7434 \cdot 10^{-5} \cdot x^2 \cdot y^2$$
$$+1.4099 \cdot 10^{-5} \cdot x \cdot y^3 - 6.9841 \cdot 10^{-6} \cdot y^4 + 0.0070436 \cdot x^3 - 0.017525 \cdot x^2 \cdot y$$
$$+0.0075661 \cdot x \cdot y^2 - 0.0032238 \cdot y^3 - 1.3437 \cdot x^2 + 1.4591 \cdot x \cdot y - 0.60509 \cdot y^2$$
$$+82.8196 \cdot x - 55.8141 \cdot y - 2024.8087 \quad \text{(B.20)}$$

$$W_{x_{Day11}} = -5.3286 \cdot 10^{-5} \cdot x^4 + 0.0001115 \cdot x^3 \cdot y - 0.00013428 \cdot x^2 \cdot y^2$$
$$+2.1731 \cdot 10^{-5} \cdot x \cdot y^3 + 1.3992 \cdot 10^{-6} \cdot y^4 + 0.02221 \cdot x^3 - 0.039776 \cdot x^2 \cdot y$$
$$+0.017075 \cdot x \cdot y^2 - 0.00049926 \cdot y^3 - 3.3561 \cdot x^2 + 3.2049 \cdot x \cdot y - 0.42399 \cdot y^2$$
$$+188.7735 \cdot x - 68.1278 \cdot y - 3309.7683 \quad \text{(B.21)}$$

$$W_{y_{Day11}} = -6.2138 \cdot 10^{-6} \cdot x^4 + 0.00015741 \cdot x^3 \cdot y - 6.4567 \cdot 10^{-5} \cdot x^2 \cdot y^2$$
$$-4.8524 \cdot 10^{-7} \cdot x \cdot y^3 - 6.6551 \cdot 10^{-6} \cdot y^4 + 0.016527 \cdot x^3 - 0.030976 \cdot x^2 \cdot y$$
$$+0.0060651 \cdot x \cdot y^2 - 0.0029623 \cdot y^3 - 2.4549 \cdot x^2 + 1.8463 \cdot x \cdot y - 0.60976 \cdot y^2$$
$$+120.9342 \cdot x - 65.0783 \cdot y - 2646.1914 \quad \text{(B.22)}$$

$$W_{x_{Day12}} = -0.0001175 \cdot x^4 + 0.00016796 \cdot x^3 \cdot y - 0.00015348 \cdot x^2 \cdot y^2$$
$$+5.2731 \cdot 10^{-5} \cdot x \cdot y^3 - 1.1913 \cdot 10^{-5} \cdot y^4 + 0.038296 \cdot x^3 - 0.049349 \cdot x^2 \cdot y$$
$$+0.027822 \cdot x \cdot y^2 - 0.0070709 \cdot y^3 - 4.7297 \cdot x^2 + 4.5722 \cdot x \cdot y - 1.6039 \cdot y^2$$
$$+264.1071 \cdot x - 160.6905 \cdot y - 6145.988 \quad \text{(B.23)}$$

$$W_{y_{Day12}} = -7.769 \cdot 10^{-5} \cdot x^4 + 0.00013676 \cdot x^3 \cdot y - 7.1359 \cdot 10^{-5} \cdot x^2 \cdot y^2$$
$$+4.9292 \cdot 10^{-5} \cdot x \cdot y^3 - 9.5847 \cdot 10^{-6} \cdot y^4 + 0.025612 \cdot x^3 - 0.030452 \cdot x^2 \cdot y$$
$$+0.021211 \cdot x \cdot y^2 - 0.0058154 \cdot y^3 - 2.9517 \cdot x^2 + 3.2918 \cdot x \cdot y - 1.281 \cdot y^2$$
$$+178.1346 \cdot x - 123.8493 \cdot y - 4492.6457 \quad \text{(B.24)}$$

$$
\begin{aligned}
W_{x_{Day13}} &= -0.00021493 \cdot x^4 + 9.2015 \cdot 10^{-5} \cdot x^3 \cdot y - 0.00012107 \cdot x^2 \cdot y^2 \\
&\quad +3.7881 \cdot 10^{-5} \cdot x \cdot y^3 - 9.3913 \cdot 10^{-6} \cdot y^4 + 0.045164 \cdot x^3 - 0.03376 \cdot x^2 \cdot y \\
&\quad +0.020219 \cdot x \cdot y^2 - 0.0054323 \cdot y^3 - 4.2892 \cdot x^2 + 3.1697 \cdot x \cdot y - 1.1939 \cdot y^2 \\
&\quad +204.5747 \cdot x - 114.4608 \cdot y - 4420.3994 \qquad \text{(B.25)}
\end{aligned}
$$

$$
\begin{aligned}
W_{y_{Day13}} &= -8.873 \cdot 10^{-5} \cdot x^4 + 0.00014428 \cdot x^3 \cdot y - 5.5704 \cdot 10^{-5} \cdot x^2 \cdot y^2 \\
&\quad +4.9216 \cdot 10^{-5} \cdot x \cdot y^3 - 2.8959 \cdot 10^{-6} \cdot y^4 + 0.028656 \cdot x^3 - 0.027489 \cdot x^2 \cdot y \\
&\quad +0.018957 \cdot x \cdot y^2 - 0.0030489 \cdot y^3 - 2.9909 \cdot x^2 + 2.8247 \cdot x \cdot y - 0.79856 \cdot y^2 \\
&\quad +160.2668 \cdot x - 83.4189 \cdot y - 3259.6748 \qquad \text{(B.26)}
\end{aligned}
$$

$$
\begin{aligned}
W_{x_{Day14}} &= -0.00013272 \cdot x^4 + 7.7186 \cdot 10^{-5} \cdot x^3 \cdot y - 9.1802 \cdot 10^{-5} \cdot x^2 \cdot y^2 \\
&\quad +4.4348 \cdot 10^{-6} \cdot x \cdot y^3 - 7.0222 \cdot 10^{-6} \cdot y^4 + 0.031401 \cdot x^3 - 0.025963 \cdot x^2 \cdot y \\
&\quad +0.0081281 \cdot x \cdot y^2 - 0.0031269 \cdot y^3 - 3.1608 \cdot x^2 + 1.7019 \cdot x \cdot y - 0.61439 \cdot y^2 \\
&\quad +131.6839 \cdot x - 58.2386 \cdot y - 2428.7145 \qquad \text{(B.27)}
\end{aligned}
$$

$$
\begin{aligned}
W_{y_{Day14}} &= -6.4978 \cdot 10^{-5} \cdot x^4 + 0.00012477 \cdot x^3 \cdot y + 5.1963 \cdot 10^{-6} \cdot x^2 \cdot y^2 \\
&\quad +2.7518 \cdot 10^{-5} \cdot x \cdot y^3 + 1.6633 \cdot 10^{-5} \cdot y^4 + 0.022063 \cdot x^3 - 0.013564 \cdot x^2 \cdot y \\
&\quad +0.0077793 \cdot x \cdot y^2 + 0.0054717 \cdot y^3 - 1.9091 \cdot x^2 + 1.2205 \cdot x \cdot y + 0.63068 \cdot y^2 \\
&\quad +82.5344 \cdot x + 24.4327 \cdot y - 133.7519 \qquad \text{(B.28)}
\end{aligned}
$$

$$
\begin{aligned}
W_{x_{Day15}} &= -9.9881 \cdot 10^{-5} \cdot x^4 + 1.0584 \cdot 10^{-5} \cdot x^3 \cdot y - 0.00011508 \cdot x^2 \cdot y^2 \\
&\quad -3.059 \cdot 10^{-7} \cdot x \cdot y^3 - 1.5218 \cdot 10^{-5} \cdot y^4 + 0.01735 \cdot x^3 - 0.022661 \cdot x^2 \cdot y \\
&\quad +0.008934 \cdot x \cdot y^2 - 0.0061201 \cdot y^3 - 2.0388 \cdot x^2 + 1.7184 \cdot x \cdot y - 1.0592 \cdot y^2 \\
&\quad +103.5155 \cdot x - 87.3026 \cdot y - 2885.4806 \qquad \text{(B.29)}
\end{aligned}
$$

$$
\begin{aligned}
W_{y_{Day15}} &= -1.4499 \cdot 10^{-5} \cdot x^4 + 5.0784 \cdot 10^{-5} \cdot x^3 \cdot y + 2.2462 \cdot 10^{-5} \cdot x^2 \cdot y^2 \\
&+7.3164 \cdot 10^{-5} \cdot x \cdot y^3 + 1.4495 \cdot 10^{-5} \cdot y^4 + 0.0062814 \cdot x^3 - 0.0016042 \cdot x^2 \cdot y \\
&+0.019971 \cdot x \cdot y^2 + 0.0015203 \cdot y^3 - 0.394 \cdot x^2 + 1.971 \cdot x \cdot y - 0.38649 \cdot y^2 \\
&+69.3625 \cdot x - 64.2212 \cdot y - 2465.694 \qquad \text{(B.30)}
\end{aligned}
$$

$$
\begin{aligned}
W_{x_{Day16}} &= -0.00016715 \cdot x^4 - 3.9091 \cdot 10^{-5} \cdot x^3 \cdot y - 5.8434 \cdot 10^{-5} \cdot x^2 \cdot y^2 \\
&+5.0229 \cdot 10^{-6} \cdot x \cdot y^3 - 1.4263 \cdot 10^{-5} \cdot y^4 + 0.023817 \cdot x^3 - 0.0074968 \cdot x^2 \cdot y \\
&+0.0061798 \cdot x \cdot y^2 - 0.0059486 \cdot y^3 - 1.8009 \cdot x^2 + 0.95215 \cdot x \cdot y - 0.99203 \cdot y^2 \\
&+78.5483 \cdot x - 75.6386 \cdot y - 2484.8457 \qquad \text{(B.31)}
\end{aligned}
$$

$$
\begin{aligned}
W_{y_{Day16}} &= -1.9209 \cdot 10^{-5} \cdot x^4 + 4.4523 \cdot 10^{-5} \cdot x^3 \cdot y + 2.3677 \cdot 10^{-5} \cdot x^2 \cdot y^2 \\
&+6.33 \cdot 10^{-5} \cdot x \cdot y^3 - 1.1301 \cdot 10^{-5} \cdot y^4 + 0.007557 \cdot x^3 - 0.0013449 \cdot x^2 \cdot y \\
&+0.017066 \cdot x \cdot y^2 - 0.0074095 \cdot y^3 - 0.57311 \cdot x^2 + 1.7127 \cdot x \cdot y - 1.4881 \cdot y^2 \\
&+69.7143 \cdot x - 121.0077 \cdot y - 3560.4667 \qquad \text{(B.32)}
\end{aligned}
$$

$$
\begin{aligned}
W_{x_{Day17}} &= -7.2911 \cdot 10^{-5} \cdot x^4 - 2.6615 \cdot 10^{-6} \cdot x^3 \cdot y - 9.0812 \cdot 10^{-5} \cdot x^2 \cdot y^2 \\
&-1.5858 \cdot 10^{-5} \cdot x \cdot y^3 - 7.3305 \cdot 10^{-6} \cdot y^4 + 0.012864 \cdot x^3 - 0.018154 \cdot x^2 \cdot y \\
&+0.0028038 \cdot x \cdot y^2 - 0.0023934 \cdot y^3 - 1.728 \cdot x^2 + 1.0696 \cdot x \cdot y - 0.41149 \cdot y^2 \\
&+83.6581 \cdot x - 40.5901 \cdot y - 1751.6326 \qquad \text{(B.33)}
\end{aligned}
$$

$$
\begin{aligned}
W_{y_{Day17}} &= 1.6704 \cdot 10^{-5} \cdot x^4 + 8.3918 \cdot 10^{-5} \cdot x^3 \cdot y + 2.1902 \cdot 10^{-5} \cdot x^2 \cdot y^2 \\
&+1.6203 \cdot 10^{-5} \cdot x \cdot y^3 + 1.2885 \cdot 10^{-5} \cdot y^4 + 0.0049748 \cdot x^3 - 0.0060427 \cdot x^2 \cdot y \\
&+0.0038792 \cdot x \cdot y^2 + 0.0041837 \cdot y^3 - 0.59976 \cdot x^2 + 0.66274 \cdot x \cdot y + 0.46075 \cdot y^2 \\
&+37.5986 \cdot x + 15.0083 \cdot y - 143.1067 \qquad \text{(B.34)}
\end{aligned}
$$

$$
W_{x_{Day18}} = -4.5055 \cdot 10^{-5} \cdot x^4 - 1.2877 \cdot 10^{-5} \cdot x^3 \cdot y - 3.5389 \cdot 10^{-5} \cdot x^2 \cdot y^2
$$

$$+8.3305 \cdot 10^{-6} \cdot x \cdot y^3 - 3.0034 \cdot 10^{-6} \cdot y^4 + 0.0089429 \cdot x^3 - 0.005908 \cdot x^2 \cdot y$$
$$+0.0056053 \cdot x \cdot y^2 - 0.0016245 \cdot y^3 - 1.0122 \cdot x^2 + 0.84314 \cdot x \cdot y - 0.3602 \cdot y^2$$
$$+59.6307 \cdot x - 34.9633 \cdot y - 1419.981 \quad \text{(B.35)}$$

$$W_{y_{Day18}} = 4.5263 \cdot 10^{-5} \cdot x^4 + 6.8649 \cdot 10^{-5} \cdot x^3 \cdot y - 1.9669 \cdot 10^{-5} \cdot x^2 \cdot y^2$$
$$+5.1025 \cdot 10^{-6} \cdot x \cdot y^3 - 7.5763 \cdot 10^{-6} \cdot y^4 - 0.00066672 \cdot x^3 - 0.012476 \cdot x^2 \cdot y$$
$$+0.0043985 \cdot x \cdot y^2 - 0.0033345 \cdot y^3 - 0.60493 \cdot x^2 + 1.0255 \cdot x \cdot y - 0.6272 \cdot y^2$$
$$+52.1485 \cdot x - 58.1157 \cdot y - 1998.7178 \quad \text{(B.36)}$$

$$W_{x_{Day19}} = 9.0853 \cdot 10^{-5} \cdot x^4 - 4.0829 \cdot 10^{-5} \cdot x^3 \cdot y - 6.1571 \cdot 10^{-5} \cdot x^2 \cdot y^2$$
$$+2.2427 \cdot 10^{-6} \cdot x \cdot y^3 - 4.1046 \cdot 10^{-6} \cdot y^4 - 0.013515 \cdot x^3 - 0.007707 \cdot x^2 \cdot y$$
$$+0.0058267 \cdot x \cdot y^2 - 0.0017878 \cdot y^3 + 0.083597 \cdot x^2 + 0.93952 \cdot x \cdot y$$
$$-0.3797 \cdot y^2 + 38.9585 \cdot x - 37.0276 \cdot y - 1315.0686 \quad \text{(B.37)}$$

$$W_{y_{Day19}} = 8.7565 \cdot 10^{-5} \cdot x^4 + 8.8087 \cdot 10^{-5} \cdot x^3 \cdot y + 1.1904 \cdot 10^{-5} \cdot x^2 \cdot y^2$$
$$+3.8816 \cdot 10^{-5} \cdot x \cdot y^3 - 7.2158 \cdot 10^{-6} \cdot y^4 - 0.0053764 \cdot x^3 - 0.0086026 \cdot x^2 \cdot y$$
$$+0.011463 \cdot x \cdot y^2 - 0.0046055 \cdot y^3 - 0.16435 \cdot x^2 + 1.5006 \cdot x \cdot y$$
$$-0.95902 \cdot y^2 + 54.632 \cdot x - 85.0967 \cdot y - 2634.428 \quad \text{(B.38)}$$

$$W_{x_{Day02}} = 4.7217 \cdot 10^{-5} \cdot x^4 - 3.5854 \cdot 10^{-5} \cdot x^3 \cdot y - 5.0711 \cdot 10^{-5} \cdot x^2 \cdot y^2$$
$$+1.4171 \cdot 10^{-7} \cdot x \cdot y^3 + 1.8008 \cdot 10^{-6} \cdot y^4 - 0.0052925 \cdot x^3 - 0.0055116 \cdot x^2 \cdot y$$
$$+0.0041893 \cdot x \cdot y^2 + 0.00076597 \cdot y^3 - 0.29848 \cdot x^2 + 0.6481 \cdot x \cdot y$$
$$+0.045663 \cdot y^2 + 37.2788 \cdot x - 4.4475 \cdot y - 468.6249 \quad \text{(B.39)}$$

$$W_{y_{Day02}} = 9.4178 \cdot 10^{-6} \cdot x^4 + 0.00011938 \cdot x^3 \cdot y + 3.7352 \cdot 10^{-6} \cdot x^2 \cdot y^2$$
$$+1.7129 \cdot 10^{-6} \cdot x \cdot y^3 - 6.1765 \cdot 10^{-6} \cdot y^4 + 0.0096418 \cdot x^3 - 0.013775 \cdot x^2 \cdot y$$
$$+0.00035883 \cdot x \cdot y^2 - 0.0022207 \cdot y^3 - 1.2401 \cdot x^2 + 0.54111 \cdot x \cdot y$$
$$-0.29001 \cdot y^2 + 47.2142 \cdot x - 21.2676 \cdot y - 785.5908 \quad \text{(B.40)}$$

$$
\begin{aligned}
W_{x_{Day21}} &= 7.3063 \cdot 10^{-5} \cdot x^4 - 5.7388 \cdot 10^{-5} \cdot x^3 \cdot y - 3.5903 \cdot 10^{-5} \cdot x^2 \cdot y^2 \\
&\quad -3.1865 \cdot 10^{-6} \cdot x \cdot y^3 - 3.5396 \cdot 10^{-6} \cdot y^4 - 0.010539 \cdot x^3 + 0.00094943 \cdot x^2 \cdot y \\
&\quad +0.0020511 \cdot x \cdot y^2 - 0.0011799 \cdot y^3 + 0.30502 \cdot x^2 + 0.15513 \cdot x \cdot y \\
&\quad -0.19263 \cdot y^2 + 5.57 \cdot x - 12.8699 \cdot y - 356.6895 \qquad \text{(B.41)}
\end{aligned}
$$

$$
\begin{aligned}
W_{y_{Day21}} &= 4.7456 \cdot 10^{-5} \cdot x^4 + 0.00010301 \cdot x^3 \cdot y + 2.1685 \cdot 10^{-5} \cdot x^2 \cdot y^2 \\
&\quad +2.8547 \cdot 10^{-5} \cdot x \cdot y^3 - 3.2161 \cdot 10^{-6} \cdot y^4 + 0.0013148 \cdot x^3 - 0.0082066 \cdot x^2 \cdot y \\
&\quad +0.0064915 \cdot x \cdot y^2 - 0.0024959 \cdot y^3 - 0.45296 \cdot x^2 + 0.87846 \cdot x \cdot y - \\
&\quad 0.50317 \cdot y^2 + 36.4977 \cdot x - 42.4316 \cdot y - 1268.5899 \qquad \text{(B.42)}
\end{aligned}
$$

$$
\begin{aligned}
W_{x_{Day22}} &= 2.5916 \cdot 10^{-5} \cdot x^4 - 8.9653 \cdot 10^{-5} \cdot x^3 \cdot y + 8.6059 \cdot 10^{-5} \cdot x^2 \cdot y^2 \\
&\quad -4.7051 \cdot 10^{-6} \cdot x \cdot y^3 + 1.9127 \cdot 10^{-6} \cdot y^4 - 0.0068668 \cdot x^3 + 0.027523 \cdot x^2 \cdot y \\
&\quad -0.0086061 \cdot x \cdot y^2 + 0.00087467 \cdot y^3 + 1.3255 \cdot x^2 - 1.9331 \cdot x \cdot y \\
&\quad +0.28718 \cdot y^2 - 85.5287 \cdot x + 42.3766 \cdot y + 1728.2181 \qquad \text{(B.43)}
\end{aligned}
$$

$$
\begin{aligned}
W_{y_{Day22}} &= -1.062 \cdot 10^{-5} \cdot x^4 + 9.7302 \cdot 10^{-6} \cdot x^3 \cdot y + 3.2423 \cdot 10^{-5} \cdot x^2 \cdot y^2 \\
&\quad -4.8133 \cdot 10^{-5} \cdot x \cdot y^3 - 1.0742 \cdot 10^{-5} \cdot y^4 + 0.0018599 \cdot x^3 + 0.0053387 \cdot x^2 \cdot y \\
&\quad -0.016597 \cdot x \cdot y^2 - 0.0013229 \cdot y^3 + 0.18181 \cdot x^2 - 1.8151 \cdot x \cdot y \\
&\quad +0.28385 \cdot y^2 - 62.791 \cdot x + 51.4003 \cdot y + 2036.3143 \qquad \text{(B.44)}
\end{aligned}
$$

$$
\begin{aligned}
W_{x_{Day23}} &= 5.6777 \cdot 10^{-7} \cdot x^4 - 9.7596 \cdot 10^{-5} \cdot x^3 \cdot y + 2.659 \cdot 10^{-5} \cdot x^2 \cdot y^2 \\
&\quad -3.2542 \cdot 10^{-5} \cdot x \cdot y^3 + 7.6599 \cdot 10^{-6} \cdot y^4 - 0.0035656 \cdot x^3 + 0.015836 \cdot x^2 \cdot y \\
&\quad -0.012178 \cdot x \cdot y^2 + 0.0041818 \cdot y^3 + 0.52953 \cdot x^2 - 1.7661 \cdot x \cdot y \\
&\quad +0.8415 \cdot y^2 - 56.4218 \cdot x + 75.5582 \cdot y + 2209.6836 \qquad \text{(B.45)}
\end{aligned}
$$

$$
\begin{aligned}
W_{y_{Day23}} &= 3.3912 \cdot 10^{-5} \cdot x^4 + 4.5455 \cdot 10^{-5} \cdot x^3 \cdot y + 4.5035 \cdot 10^{-5} \cdot x^2 \cdot y^2 \\
&\quad -2.8944 \cdot 10^{-5} \cdot x \cdot y^3 r + 2.0763 \cdot 10^{-5} \cdot y^4 - 0.0019676 \cdot x^3 + 0.0027564 \cdot x^2 \cdot y \\
&\quad -0.01095 \cdot x \cdot y^2 + 0.010181 \cdot y^3 + 0.23792 \cdot x^2 - 1.0593 \cdot x \cdot y + 1.7724 \cdot y^2 \\
&\quad -35.8895 \cdot x + 128.3268 \cdot y + 3318.4812 \qquad \text{(B.46)}
\end{aligned}
$$

$$
\begin{aligned}
W_{x_{Day24}} &= 0.00011509 \cdot x^4 + 1.2696 \cdot 10^{-5} \cdot x^3 \cdot y - 4.4244 \cdot 10^{-5} \cdot x^2 \cdot y^2 \\
&\quad -2.4945 \cdot 10^{-5} \cdot x \cdot y^3 - 1.1563 \cdot 10^{-5} \cdot y^4 - 0.010333 \cdot x^3 - 0.010063 \cdot x^2 \cdot y \\
&\quad -0.0032369 \cdot x \cdot y^2 - 0.0036626 \cdot y^3 - 0.32989 \cdot x^2 + 0.16131 \cdot x \cdot y \\
&\quad -0.48041 \cdot y^2 + 28.4321 \cdot x - 33.6105 \cdot y - 1162.7586 \qquad \text{(B.47)}
\end{aligned}
$$

$$
\begin{aligned}
W_{y_{Day24}} &= -4.538 \cdot 10^{-5} \cdot x^4 + 3.9327 \cdot 10^{-5} \cdot x^3 \cdot y + 4.9805 \cdot 10^{-5} \cdot x^2 \cdot y^2 \\
&\quad +5.391 \cdot 10^{-5} \cdot x \cdot y^3 + 2.8808 \cdot 10^{-5} \cdot y^4 + 0.0099366 \cdot x^3 + 0.0038542 \cdot x^2 \cdot y \\
&\quad +0.011768 \cdot x \cdot y^2 + 0.0084575 \cdot y^3 - 0.3999 \cdot x^2 + 0.97156 \cdot x \cdot y \\
&\quad +0.86022 \cdot y^2 + 39.5227 \cdot x + 32.2481 \cdot y + 151.2942 \qquad \text{(B.48)}
\end{aligned}
$$

$$
\begin{aligned}
W_{x_{Day25}} &= 0.00017423 \cdot x^4 - 4.3332 \cdot 10^{-6} \cdot x^3 \cdot y - 4.9328 \cdot 10^{-5} \cdot x^2 \cdot y^2 \\
&\quad -2.0136 \cdot 10^{-6} \cdot x \cdot y^3 - 1.4844 \cdot 10^{-5} \cdot y^4 - 0.021904 \cdot x^3 - 0.0088655 \cdot x^2 \cdot y \\
&\quad +0.0040999 \cdot x \cdot y^2 - 0.0057258 \cdot y^3 + 0.44384 \cdot x^2 + 0.82603 \cdot x \cdot y \\
&\quad -0.90678 \cdot y^2 + 28.6667 \cdot x - 68.1475 \cdot y - 1943.6042 \qquad \text{(B.49)}
\end{aligned}
$$

$$
\begin{aligned}
W_{y_{Day25}} &= -3.8209 \cdot 10^{-5} \cdot x^4 + 2.5302 \cdot 10^{-5} \cdot x^3 \cdot y + 1.9358 \cdot 10^{-5} \cdot x^2 \cdot y^2 \\
&\quad +5.2394 \cdot 10^{-5} \cdot x \cdot y^3 - 3.7454 \cdot 10^{-7} \cdot y^4 + 0.0079339 \cdot x^3 - 0.00028776 \cdot x^2 \cdot y \\
&\quad +0.013749 \cdot x \cdot y^2 - 0.0035116 \cdot y^3 - 0.49712 \cdot x^2 + 1.3388 \cdot x \cdot y - 0.9792 \cdot y^2 \\
&\quad +54.8292 \cdot x - 92.2827 \cdot y - 2964.0904 \qquad \text{(B.50)}
\end{aligned}
$$

$$
W_{x_{Day26}} = 8.1124 \cdot 10^{-5} \cdot x^4 + 3.3843 \cdot 10^{-5} \cdot x^3 \cdot y + 2.1724 \cdot 10^{-5} \cdot x^2 \cdot y^2
$$

$$+2.6298 \cdot 10^{-5} \cdot x \cdot y^3 r + 1.7515 \cdot 10^{-6} \cdot y^4 - 0.0044217 \cdot x^3 - 0.00011074 \cdot x^2 \cdot y$$
$$+0.0063394 \cdot x \cdot y^2 - 0.00034745 \cdot y^3 - 0.12323 \cdot x^2 + 0.65222 \cdot x \cdot y$$
$$-0.18428 \cdot y^2 + 34.4348 \cdot x - 21.2727 \cdot y - 911.5867 \quad \text{(B.51)}$$

$$W_{y_{Day26}} = 3.4854 \cdot 10^{-6} \cdot x^4 - 1.3876 \cdot 10^{-5} \cdot x^3 \cdot y - 3.8074 \cdot 10^{-5} \cdot x^2 \cdot y^2$$
$$+2.1963 \cdot 10^{-6} \cdot x \cdot y^3 - 4.0304 \cdot 10^{-5} \cdot y^4 - 0.0016648 \cdot x^3 - 0.006851 \cdot x^2 \cdot y$$
$$+0.0044427 \cdot x \cdot y^2 - 0.016395 \cdot y^3 - 0.29966 \cdot x^2 + 0.82789 \cdot x \cdot y$$
$$-2.5301 \cdot y^2 + 40.2538 \cdot x - 175.4348 \cdot y - 4602.505 \quad \text{(B.52)}$$

$$W_{x_{Day27}} = 8.4143 \cdot 10^{-5} \cdot x^4 + 9.8945 \cdot 10^{-5} \cdot x^3 \cdot y + 3.8466 \cdot 10^{-5} \cdot x^2 \cdot y^2$$
$$-1.3044 \cdot 10^{-5} \cdot x \cdot y^3 + 7.7583 \cdot 10^{-6} \cdot y^4 - 0.0010764 \cdot x^3 - 0.0056955 \cdot x^2 \cdot y$$
$$-0.0065899 \cdot x \cdot y^2 + 0.003485 \cdot y^3 - 0.5262 \cdot x^2 - 0.35392 \cdot x \cdot y$$
$$+0.60775 \cdot y^2 + 12.8735 \cdot x + 40.6902 \cdot y + 715.094 \quad \text{(B.53)}$$

$$W_{y_{Day27}} = 1.2726 \cdot 10^{-6} \cdot x^4 + 3.2744 \cdot 10^{-5} \cdot x^3 \cdot y + 2.2391 \cdot 10^{-6} \cdot x^2 \cdot y^2$$
$$-6.1077 \cdot 10^{-5} \cdot x \cdot y^3 - 1.0465 \cdot 10^{-5} \cdot y^4 + 0.0036918 \cdot x^3 - 0.0038779 \cdot x^2 \cdot y$$
$$-0.016528 \cdot x \cdot y^2 - 0.00091973 \cdot y^3 - 0.47103 \cdot x^2 - 1.2627 \cdot x \cdot y$$
$$+0.28064 \cdot y^2 - 20.5261 \cdot x + 38.1963 \cdot y + 1144.3687 \quad \text{(B.54)}$$

$$W_{x_{Day28}} = 9.8377 \cdot 10^{-5} \cdot x^4 + 6.5085 \cdot 10^{-5} \cdot x^3 \cdot y - 1.6686 \cdot 10^{-5} \cdot x^2 \cdot y^2$$
$$+5.312 \cdot 10^{-6} \cdot x \cdot y^3 + 9.3803 \cdot 10^{-6} \cdot y^4 - 0.0068068 \cdot x^3 - 0.01318 \cdot x^2 \cdot y$$
$$+0.0036787 \cdot x \cdot y^2 + 0.0030943 \cdot y^3 - 0.55767 \cdot x^2 + 1.0077 \cdot x \cdot y$$
$$+0.29665 \cdot y^2 + 59.0514 \cdot x - 0.8175 \cdot y - 806.9604 \quad \text{(B.55)}$$

$$W_{y_{Day28}} = 1.9073 \cdot 10^{-5} \cdot x^4 + 2.4467 \cdot 10^{-5} \cdot x^3 \cdot y - 2.322 \cdot 10^{-5} \cdot x^2 \cdot y^2$$
$$-3.1536 \cdot 10^{-5} \cdot x \cdot y^3 + 1.6263 \cdot 10^{-5} \cdot y^4 + 0.0002855 \cdot x^3 - 0.0076458 \cdot x^2 \cdot y$$
$$-0.0056293 \cdot x \cdot y^2 + 0.0074967 \cdot y^3 - 0.44746 \cdot x^2 - 0.052903 \cdot x \cdot y$$
$$+1.1362 \cdot y^2 + 17.0009 \cdot x + 66.2493 \cdot y + 1184.5847 \quad \text{(B.56)}$$

$$
\begin{aligned}
W_{x_{Day29}} &= 7.8228 \cdot 10^{-5} \cdot x^4 + 5.2999 \cdot 10^{-5} \cdot x^3 \cdot y - 4.9061 \cdot 10^{-5} \cdot x^2 \cdot y^2 \\
&+4.0694 \cdot 10^{-5} \cdot x \cdot y^3 - 1.0531 \cdot 10^{-6} \cdot y^4 - 0.0034127 \cdot x^3 - 0.018202 \cdot x^2 \cdot y \\
&+0.016062 \cdot x \cdot y^2 - 0.0026252 \cdot y^3 - 1.0639 \cdot x^2 + 2.3468 \cdot x \cdot y - 0.78943 \cdot y^2 \\
&+113.615 \cdot x - 86.6504 \cdot y - 3296.5053 \qquad \text{(B.57)}
\end{aligned}
$$

$$
\begin{aligned}
W_{y_{Day29}} &= 7.3266 \cdot 10^{-5} \cdot x^4 + 6.1535 \cdot 10^{-5} \cdot x^3 \cdot y - 5.7685 \cdot 10^{-5} \cdot x^2 \cdot y^2 \\
&+3.4278 \cdot 10^{-5} \cdot x \cdot y^3 + 1.9839 \cdot 10^{-6} \cdot y^4 - 0.0044663 \cdot x^3 - 0.018525 \cdot x^2 \cdot y \\
&+0.016509 \cdot x \cdot y^2 - 0.0012784 \cdot y^3 - 0.71044 \cdot x^2 + 2.4849 \cdot x \cdot y - 0.6442 \cdot y^2 \\
&+103.6077 \cdot x - 83.0324 \cdot y - 3196.0328 \qquad \text{(B.58)}
\end{aligned}
$$

$$
\begin{aligned}
W_{x_{Day30}} &= 2.314 \cdot 10^{-5} \cdot x^4 + 4.0245 \cdot 10^{-5} \cdot x^3 \cdot y - 4.7282 \cdot 10^{-5} \cdot x^2 \cdot y^2 \\
&+2.5332 \cdot 10^{-5} \cdot x \cdot y^3 - 2.5781 \cdot 10^{-6} \cdot y^4 + 0.0040293 \cdot x^3 - 0.016062 \cdot x^2 \cdot y \\
&+0.010831 \cdot x \cdot y^2 - 0.0024522 \cdot y^3 - 1.3575 \cdot x^2 + 1.6971 \cdot x \cdot y - 0.6197 \cdot y^2 \\
&+97.1109 \cdot x - 63.6091 \cdot y - 2460.8827 \qquad \text{(B.59)}
\end{aligned}
$$

$$
\begin{aligned}
W_{y_{Day30}} &= 4.2561 \cdot 10^{-5} \cdot x^4 + 8.8659 \cdot 10^{-5} \cdot x^3 \cdot y - 1.9445 \cdot 10^{-5} \cdot x^2 \cdot y^2 \\
&+8.9608 \cdot 10^{-7} \cdot x \cdot y^3 - 1.6394 \cdot 10^{-5} \cdot y^4 + 0.0028987 \cdot x^3 - 0.013709 \cdot x^2 \cdot y \\
&+0.0034533 \cdot x \cdot y^2 - 0.0064635 \cdot y^3 - 0.88107 \cdot x^2 + 0.97702 \cdot x \cdot y \\
&-1.0282 \cdot y^2 + 57.2653 \cdot x - 79.721 \cdot y - 2449.7878 \qquad \text{(B.60)}
\end{aligned}
$$

$$
\begin{aligned}
W_{x_{Day31}} &= 7.2831 \cdot 10^{-5} \cdot x^4 + 1.9442 \cdot 10^{-6} \cdot x^3 \cdot y - 2.7581 \cdot 10^{-5} \cdot x^2 \cdot y^2 \\
&+2.1429 \cdot 10^{-5} \cdot x \cdot y^3 - 2.213 \cdot 10^{-8} \cdot y^4 - 0.008913 \cdot x^3 - 0.0077798 \cdot x^2 \cdot y \\
&+0.0080821 \cdot x \cdot y^2 - 0.0012321 \cdot y^3 - 0.1423 \cdot x^2 + 1.1226 \cdot x \cdot y \\
&-0.38119 \cdot y^2 + 47.939 \cdot x - 41.1398 \cdot y - 1495.7159 \qquad \text{(B.61)}
\end{aligned}
$$

$$
\begin{aligned}
W_{y_{Day31}} &= 4.3529 \cdot 10^{-5} \cdot x^4 + 2.1164 \cdot 10^{-5} \cdot x^3 \cdot y - 1.2068 \cdot 10^{-5} \cdot x^2 \cdot y^2 \\
&\quad +2.3868 \cdot 10^{-5} \cdot x \cdot y^3 - 9.2715 \cdot 10^{-6} \cdot y^4 - 0.0037973 \cdot x^3 - 0.004628 \cdot x^2 \cdot y \\
&\quad +0.0091585 \cdot x \cdot y^2 - 0.0048256 \cdot y^3 - 0.069643 \cdot x^2 + 1.1495 \cdot x \cdot y \\
&\quad -0.93754 \cdot y^2 + 41.8673 \cdot x - 78.7394 \cdot y - 2355.6246 \qquad \text{(B.62)}
\end{aligned}
$$